Korean Journal of Chemical Engineering
https://doi.org/10.1007/s11814-026-00704-4

ORIGINAL ARTICLE

Synergistic Antitumor Effects of Paclitaxel Combined with PDE5 Inhibitor Avanafil on Glioma U373 Cells

Havva Aybek[1] · Mahinur Kırıcı[2] · Kubra Koc[3] · Burak Tüzün[4] · Ramazan Gündoğdu[1] · Mehmet Kadir Erdoğan[5]

Received: 26 September 2025 / Revised: 28 February 2026 / Accepted: 7 March 2026
© The Author(s) 2026

Abstract

Paclitaxel is a well-known chemotherapeutic agent that induces cancer cell death by stabilising microtubules. Avanafil, a phosphodiesterase type 5 (PDE5) inhibitor typically used for erectile dysfunction, has recently been proposed to enhance blood-brain barrier permeability. This research focuses on, for the first time, the role of avanafil used together with paclitaxel to treat glioma. The cytotoxic effect of this combination on the U373 brain cancer cell was evaluated using MTT, colony survival analysis, and wound healing assay. Western blot analyses of the agents were conducted to investigate their effects on p53, Cas-3, Cas-9, Bax, Bcl-2, and c-PARP proteins. Additionally, Avanafil, Paclitaxel, and Avanafil+Paclitaxel combinations were calculated using the Gaussian package program at the B3LYP, HF, and M062x levels in the 6–31 g, 6–31++g, and 6–31++g(d, p) basis sets. The activities of the agents against brain tumour proteins (PDB ID: 2DME and 6YPE) were compared and their ADME/T properties were also investigated. MTT and colony survival analysis demonstrated that the combination significantly inhibited U373 cell viability and proliferation. Wound healing and Western blot assays indicated impaired migration and altered expression of apoptosis-related proteins. Molecular docking and DFT analyses supported the experimental findings, and ADME/T profiling suggested favourable pharmacokinetics. Our results indicate that avanafil enhances the cytotoxicity of paclitaxel via non-apoptotic mechanisms, highlighting its potential as an adjuvant in glioma therapy.

Keywords Paclitaxel · Avanafil · U373 · Brain tumor, Molecular docking

Introduction

Among the major brain tumours, malignant glioma is the most frequently occurring type, with an annual incidence of 5/100,000 individuals [1]. As indicated by estimated data, an examination of global cancer statistics for 2018 reveals that 18.1 million individuals were diagnosed with cancer and 9.6 million died from the disease [2]. Brain cancer is a disease that requires urgent and effective treatment strategies due to its high mortality rate and limited treatment options [3]. As glioblastoma or malignant glioma is the most widespread and aggressive principal tumour in mature individuals, metastasis to other organs accelerates death and reduces the survival rate [4]. Primary central nervous system (CNS) malignancies constitute 1.4% of all cancers [5]. These tumours, which can occur in the central nervous system as either primary (primary) or secondary (metastatic) sources, reduce patients' survival time. The global annual incidence of primary malignant brain tumours is approximately 24,000 cases. Although diagnostic tools

✉ Kubra Koc
kubrakc@hotmail.com

✉ Burak Tüzün
theburaktuzun@yahoo.com

1 Department of Pharmacy Services, Vocational School of Health Services, Bingol University, Bingöl, Turkey

2 Department of Chemistry, Faculty of Arts and Sciences, Bingol University, Bingöl, Turkey

3 Department of Biology, Faculty of Science, Atatürk University, Erzurum, Turkey

4 Plant and Animal Production Department, Technical Sciences Vocational School of Sivas, Sivas Cumhuriyet University, Sivas, Turkey

5 Department of Molecular Biology and Genetics, Faculty of Arts and Sciences, Bingol University, Bingöl, Turkey

Published online: 23 March 2026

and therapeutic pathways have been developed, the treatment of brain tumours is still seen as a challenging process [6]. Chemotherapeutic drugs transported through the blood must traverse the blood vessel barrier and penetrate the maximum number of tumour cells to be effective. Since the local microenvironment of the brain can prevent the effectiveness of drugs on primary and secondary brain tumours, drugs must also cope with the resistance mechanisms in the tumour cell microenvironment [7, 8]. To date, around 120 different types of brain tumour have been identified, and different research groups have classified them according to various criteria. Today, many health institutions use the classification system recommended by the World Health Organisation (WHO). In this classification system, brain tumours are named according to the cell origin from which they are derived, the rate of tumour proliferation, from the least aggressive (benign) to the most aggressive (malignant), and their location. The most common primary CNS tumours in humans are gliomas, which are derived from glial cells that perform supportive functions in the brain. Gliomas are classified according to the cell types from which they originate, the tumour's degree of aggressiveness, and its location [9, 10]. A comprehensive understanding of the principal pathways involved in brain tumours biology and the identification of important targets is crucial. Since these patients have an extremely low survival rate compared to other cancer cases, more effective and less toxic treatments are required [11]. In healthy cell homeostasis, chronic stress triggers irreversible cell damage and death due to insufficient adaptive responses [12]. Apoptotic cell death is a fundamental process that eliminates damaged cells, maintains tissue homeostasis, and recycles cellular components that support further growth and differentiation [13]. While the expression of anti-apoptotic proteins provides a vital physiological mechanism for protecting cells against damage, these proteins also contribute to tumorigenesis in several malignancies. The induction of apoptosis constitutes a central mechanism through which radiation and cytotoxic agents exert their anti-tumor effects. However, malignant gliomas are characterized by an inherent resistance to apoptotic cell death, which is believed to be a core mechanism by which these tumors evade elimination under both conventional and targeted therapies [14]. Thus, targeting apoptotic pathways has become a key focus in the development of novel anti-glioma therapies. Apart from their classical cytotoxic effects, chemotherapy agents also display substantial effects in the immune microenvironment of the tumour. Chemotherapy agents are capable of inducing anti-tumour immune responses through the promotion of senescence-associated signal release, reduction of immune-suppressive factors, and modulation of immune-related pathways. The chemotherapy is not only capable of inducing tumour cell death through apoptosis but also of modulating immune-suppressive signals, thereby increasing the susceptibility of cancer cells to immune destruction. Due to this dual functionality, chemotherapy agents are promising candidates for combined therapy with modulators of immunity or agents increasing the permeability of the tumour to the immune response [15]. Moreover, the importance of integrating experimental findings with computational analysis has also been emphasised. In this context, the employment of quantum chemistry calculations together with in vitro cytotoxicity tests was found to provide useful information on the relationship between the electronic and structural properties of anticancer drugs and their anticancer activities. For example, high cytotoxicity activities were observed for the Zn (II)-based Schiff base coordination polymer complexes using conventional cell death pathways like apoptosis, autophagy, or necrosis. This occurs due to the influences exerted by the molecular orbital frontier distributions, supramolecular interactions, as well as the coordination geometry [16].

Paclitaxel, known as Taxol, is an important cancer therapeutic belonging to the taxane group. Its antitumor activity is related to microtubule stability [17]. While other tubulin-binding anticancer drugs block the assembly of tubulin to microtubules, paclitaxel induces the assembly of tubulin to microtubules and prevents the disassembly of microtubules. It also blocks cell cycle progression in the G2/M phase, preventing cells from undergoing mitotic division and inhibiting cancer growth [18]. Taxol provides apoptosis of tumour cells with this mechanism of action and is used as a model anticancer drug in many cancer treatments [19]. Paclitaxel is effective against malignant gliomas and brain metastases. It has also been reported to exhibit significant anticancer activity against head, neck, breast and lung cancer, and ovarian carcinoma. Paclitaxel also appears to be effective against several other human malignancies, including leukaemia and non-small cell lung cancer [20, 21]. On the other hand, Avanafil is a drug known as a phosphodiesterase 5 (PDE5) inhibitor and used to treat erectile dysfunction (sexual impotence). It inhibits the activity of the enzyme phosphodiesterase type 5, thereby preventing its rapid action and thus maintaining an erection by increasing blood flow. It acts as a competitive inhibitor of cyclic guanosine monophosphate (cGMP) at the catalytic site of phosphodiesterase enzymes. This enzyme inhibition increases cGMP levels and decreases intracellular calcium. Activating an erection causes the production and release of nitric oxide (NO) in the penis. NO lead guanylate cyclase enzyme to produce cyclic guanosine monophosphate (cGMP). Avanafil prevents phosphodiesterase-5 from destroying cGMP; thereby, cGMP remains in the penis for longer, and the persistence of cGMP leads to a longer-lasting recurrence of blood. PDE5 is involved in the degradation of the second messenger cGMP

[22–25]. Apart from this, PDE5 inhibitors also possess antioxidant, anti-inflammatory, antiproliferative, and metabolic actions in various experiments [26]. The results suggest that PDE5 inhibitors possess anticancer activity either through their action on the cGMP-PKG signal transduction pathway or through their ineffectiveness in inhibiting ABC transporters for anticancer drugs. The safety, high tolerability, and easy availability of PDE5 inhibitors make them promising candidates to assess their role in cancer chemotherapy [27]. This implies their effectiveness as adjuvants in cancer chemotherapy, especially when used in conjunction with agents such as paclitaxel.

The objective of this research work was examining a new combination treatment method, which has been considered an alternate option in place of the existing combination chemotherapy treatment method used in brain tumours. In this regard, a novel attempt has been made in this research study to investigate the combination of avanafil and paclitaxel in glioma cells. In addition, it has been a significant task in this field of study to examine the ADME/T properties of systems comprising of Avanafil, Paclitaxel, and a combination of Avanafil and Paclitaxel. This task plays a crucial role in understanding the efficacy profile of this compound used in medical treatments [28]. The objective of this research study has been Avanafil, Paclitaxel, and a combination of Avanafil & Paclitaxel, which are 3 molecules, calculated using Gaussian Package Software corresponding to B3LYP, HF, and M062x methods in 6–31 gatomic basis sets, respectively [29–31]. Then, an attempt has been made in this regard to compare the activities of these 3 molecules regarding brain cancer proteins (2DME & 6YPE) [32, 33]. Finally, an attempt has been made in this regard to assess the ADME/T property of the molecule.

Experimental

Chemicals

Streptomycin and Dimethyl sulfoxide (DMSO) were bought from Bioshop Canada. Fetal bovine serum (FBS) and Dulbecco's modified Eagle's medium (DMEM) were bought from Gibco (Thermo Fisher Scientific). Commassy blue dye (G250), sodium azide (NaN_3), skim milk powder, luminol, ponceau S, phosphoric acid (H_3PO_4), p-coumaric acid, phenylmethylsulfonyl fluoride (PMSF), benzamidine, hexane, chloroform, sodium dodecyl sulfate, Avanafil, paclitaxel, bovine serum albumin (BSA), glycerol, glycerin, ethanol, methanol, penicillin and crystal violet were bought from Sigma Aldrich; hydrogen peroxide (H_2O_2), sodium hydroxide (NaOH), Tween-20, glycine, NP-40, bromphenol blue, β-mercaptoethanol, β-glycerophosphate, ethylenediaminetetraacetic acid (EDTA), egtazine acid (EGTA) were supplied by Merck. Primary and secondary antibodies were bought from Cell Signaling Technology. Cell death detection Elisa (CDDE) and MTT (3-(4,5-dimethylthiazol-2-yl)−2,5-diphenyltetrazolium bromide) kits were supplied by Roche. Tubulin, p53, Bax, Bcl-2, Cas-3, Cas-9, and c-PARP used in Western blot studies were supplied by Santa Cruz Biotechnology (USA). Glioma cancer cell line U373 was acquired from American type cell culturing (ATCC).

Cell Viability

The main content of the medium used in the culture of U373 cells was 10% fetal bovine serum (FBS), RPMI 1640 basal medium, and 1% penicillin/streptomycin. The cells were cultured in sterile conditions and propagated in a carbon dioxide incubator at 5% CO_2, 95% humidity, and 37 °C. Paclitaxel and avanafil stock solutions were prepared in DMSO. The viability of U373 cells was determined by MTT method (Elabscience) [34]. Briefly, 96-well microplates containing 1×10^4 cells per well were incubated with increasing concentrations of paclitaxel, avanafil at 37 °C for 24 h. Then, 10 µl of MTT reagent was introduced into each well and incubated for 4 h. In the next step, 100 µl of solubilization solution was introduced and left to incubate overnight. Colour changes associated with the formazan were determined spectrophotometrically at 450 nm using an Elisa microplate reader (SpectraMax 384 Plus, Molecular Devices, USA). The cell viability was determined according to absorbance values. The IC_{50} value of each sample was calculated, and the values were served as active doses in the subsequent steps of the study.

Clonogenic Survival Assays

Clonogenic survival experiments were conducted as stated in [35, 36]. In short, 1500 cells in the exponential phase were sown in 6-cm plates, given a 24-hour adhesion period, and then treated for three days with or without paclitaxel. Until each colony developed more than 50 cells (8–10 days), the cell media was changed every 4 days. After fixing the colonies with a 3:1 methanol/acidic acid solution, they were dyed for 15 min using 0.5% crystal violet. The number of colonies was counted per plate after letting the plates air-dry overnight. The surviving fraction was determined using the plating efficiencies of the appropriate controls.

Wound Healing Assay

In vitro, a wound-healing assay/scratch test was conducted to determine the cell migration ability [35]. A total of 4 ×

10^5 cells were plated in 6-well culture plates, and once they reached 80–90% confluency, a linear scratch was introduced by a sterile pipette tip. The detached cells were eliminated by washing with PBS, followed by treatment with SPA for 72 h. The scratch line was monitored at 0, 6, and 24 h to analyze the wound healing progression, and the images were captured with an inverted microscope (Olympus CKX 41). That images were processed with Image J software, and wound closure was evaluated by normalizing and comparing 0, 6, and 24 h images of each treatment group with control.

Western Blotting

Western blotting experiments were carried out as previously described [36]. Briefly, total protein lysates were resolved by 12% sodium dodecyl sulfate–polyacrylamide gel electrophoresis (SDS-PAGE) and transferred onto polyvinylidene difluoride (PVDF) membranes. Following transfer, membranes were blocked with 5% skim milk in TBS-T buffer (50 mM Tris-HCl, 150 mM NaCl, 0.5% Tween-20, pH 7.5) to prevent nonspecific binding. Subsequently, membranes were incubated overnight at 4 °C with the appropriate primary antibodies. After thorough washing, HRP-conjugated secondary antibodies were applied, and immunoreactive bands were detected using enhanced chemiluminescence (ECL) reagents (Amersham). Densitometric analysis of the protein bands was performed using NIH ImageJ software.

Theoretical Methods

Theoretical calculations play a crucial role in elucidating the chemical and biological properties of molecules. Numerous quantum chemical parameters can be derived through such computational approaches, providing insights into molecular reactivity and stability. In this study, quantum chemical calculations were performed using Gaussian09 Rev. D.01 and GaussView 6.0 software packages [37, 38]. Calculations were conducted using B3LYP, HF, and M06-2X methods with the 6-31G basis set. These computational approaches yielded a variety of quantum chemical descriptors, each reflecting specific chemical characteristics of the molecules under investigation. The calculated parameters are presented and interpreted as follows [39];

$$\chi = -\left(\frac{\partial \mathrm{E}}{\partial \mathrm{N}}\right)_{\upsilon(r)} = \frac{1}{2}(I + A) \cong \frac{1}{2}(E_{HOMO} + E_{LUMO})$$

$$\eta = -\left(\frac{\partial^2 \mathrm{E}}{\partial \mathrm{N}^2}\right)_{\upsilon(r)} = \frac{1}{2}(I - A) \cong -\frac{1}{2}(E_{HOMO} - E_{LUMO})$$

$$\sigma = 1/\eta \quad \omega = \chi^2/2\eta \quad \epsilon = 1/\omega$$

Molecular docking calculations were carried out to evaluate and compare the biological activities of the molecules against selected biological targets. The docking studies were performed using the Maestro molecular modeling platform (version 13.4), developed by Schrödinger [40]. The docking procedure consisted of multiple sequential steps, each involving specific preparation or configuration protocols. In the initial step, the Protein Preparation Wizard module was utilized for preprocessing and optimizing the protein structures [41]. In the next phase, the studied molecules were prepared for computational analysis. Initially, the molecular structures were optimized using the Gaussian software package and processed using the LigPrep module to prepare them for docking simulations [42]. The Glide ligand docking module was subsequently employed to investigate the interactions between the prepared ligands and the target cancer-related protein [43, 44]. All calculations were performed using the OPLS4 force field to ensure accurate molecular modeling. Finally, to evaluate the pharmacokinetic and drug-likeness properties of the studied molecules, ADME/T (Absorption, Distribution, Metabolism, Excretion, and Toxicity) analysis was conducted. The QikProp module from the Schrödinger suite was used to predict the molecular behavior in human metabolism [45]. RMSD values lower than 2 Å indicate that the docking workflow is capable of accurately predicting ligand binding orientations and therefore supports the reliability of the reported docking results.

Statistical Analysis

All statistical analyses were performed with the Graph Pad Prism 5.01 software. One-way ANOVA (Analysis of Variance) and post-hoc multiple comparison tests were applied for group comparisons, considering $p < 0.05$ as statistically significant.

Results and Discussion

Determination of Avanafil and Paclitaxel IC_{50} Dose Values in U373 Cells

In vitro cell viability analysis using U373 cell lines was performed based on the manufacturer's protocols of the MTT kit (Elabscience). Following the cultivation of cells were grown in DMEM media in an incubator at 37 °C with 5% CO_2, 1×10^4 cells, which were determined by pilot experiments, were transferred into 96-well culture dishes and incubated for 24 h. The cells were then applied with avanafil and paclitaxel. After 24 h incubation, the medium was removed and 10 µL of kit reagent was introduced to

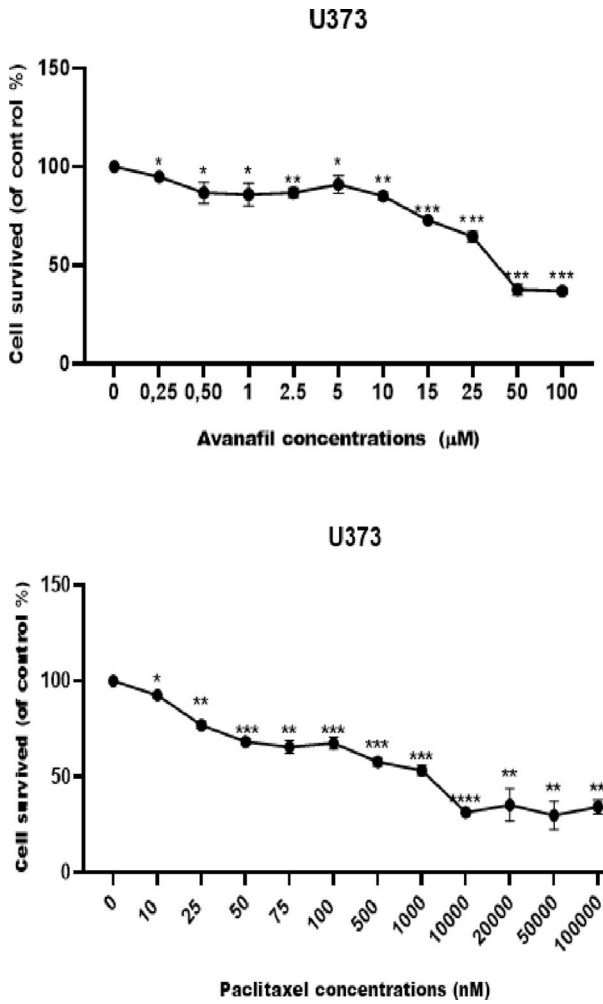

Fig. 1 Effect of increasing avanafil and paclitaxel concentration on the viability of U373 cells. 1×10^4 U373 cells were seeded in 96-well plates and treated for 24 h. Cell viability analyses were performed at 450 nm using MTT kit. *$p<0.05$; compared to control, **$p<0.01$; compared to control, ***$p<0.001$; compared to control, ****$p<0.0001$; compared to control

each well and after 4 hours of incubation, the color change was measured with a microplate reader at a wavelength of 450 nm. The proliferation percentages of the cells were calculated by subtracting the absorbance value of the treatment group from the background control and then dividing this value by the control group. MTT analysis was conducted to determine the cytotoxic effect of PDE5 inhibitor Avanafil on U373 cell line an increasing wide concentration range (0.25–100 µM). As a result of the analysis, the IC_{25} value of avanafil in U373 cells was determined as 11.7 µg/mL and the IC_{50} value was determined as 31 µg/mL. The cells were treated with paclitaxel in a wide range of increasing concentrations (10–100,000 nM) for 24 h. The IC_{25} value of paclitaxel in U373 cells was determined as 100 ng/mL and the IC_{50} value was determined as 1.5 µg/mL in Fig. 1.

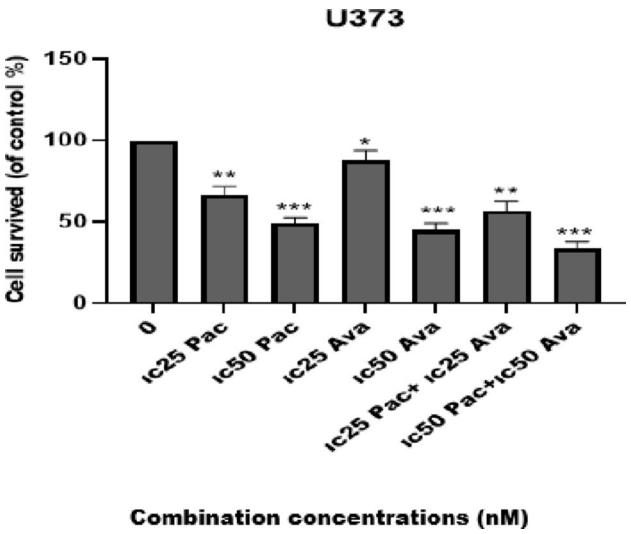

Fig. 2 Effect of paclitaxel and avanafil combination treatment on the viability of U373 cells. 1×10^4 U373 and U87 cells were seeded in 96-well plates and treated for 24 h. Cell viability analyses were performed at 450 nm using MTT kit. *$p<0.05$; compared to control, **$p<0.01$; compared to control, ***$p<0.001$; compared to control

Determination of the Effect of Avanafil and Paclitaxel Combination Treatments on the Viability of U373 Cells

The U373 cells were treated with IC_{25} paclitaxel, IC_{50} paclitaxel, IC_{25} avanafil, IC_{50} avanafil, and combination doses for 24 h. As a result of the analysis, it was determined that paclitaxel and avanafil IC_{25} and IC_{50} doses significantly reduced cell viability when compared to control cells. In particular, the combination of paclitaxel and avanafil IC_{50} was found to be more effective in reducing cell viability than mono treatments and showed a synergistic effect in Fig. 2.

It is suggested that PDE5 inhibitors enhance the cytotoxic effects of cancer cells by sensitizing them to chemotherapeutic agents through their effect on the efflux capabilities of ABC transporter proteins. Vardenafil and sildenafil, both PDE5 inhibitors, have been shown to increase the activity of docetaxel, vinblastin, and paclitaxel in HEK293 cells by blocking ABC transporters [46], while another study reported that sildenafil increased the cytotoxic effect of anticancer agents such as paclitaxel and mitoxantrone [47]. Evidence also exists suggesting that the combination of chemotherapeutic agents and PDE5 inhibitors induces apoptosis, and that this is related to increased accumulation of cellular reactive oxygen species [27]. In the A549 lung cancer tumor model, the PDE5 inhibitor exisulind, in combination with docetaxel, triggered apoptosis and increased proliferation both in vivo and in vitro [48]. In 35 different patients with metastatic breast cancer, the exisulind-capecitabine combination resulted in increased tumor suppression and apoptotic activity [49]. As with these

promising results, which demonstrate the importance of PDE5 inhibitors in adjuvant chemotherapy, our study also showed that avanafil increased the cytotoxicity of paclitaxel. We suspect that this effect is partly related to the inhibition of specific ABC transporters due to the combination therapy, and therefore we conducted further experiments to elucidate the molecular mechanism of action.

Determination of the Effects of Avanafil and Paclitaxel Treatments on Colony Survival in U373 Cells

U373 cells were introduced into 6 cm cell dishes at a density of 1.5×10^3 cells. The next day, considering the previously performed MTT experiment, U373 was treated with increasing doses of paclitaxel (25, 50, 100, 500 nM) for 24 h. U373 was treated with increasing doses of avanafil (5, 11.7, 31, 100 µM) for 24 h. In combination treatments, for U373, one group was treated with the dose of 30 nM paclitaxel dose kept constant and avanafil increasing doses (5, 8, 31, 50 µM), and the other group was treated with the dose of 8 µM avanafil dose kept constant and paclitaxel increasing doses (10, 30, 50, 100 nM) for 24 h. After the treatment, the medium of each cell group was renewed, and the colony formation of the cells was followed for 12–14 days. At the end of the process, 0.5% crystal violet staining was performed, followed by colony analyses. As a result of the analysis, it was determined that increasing doses of paclitaxel treatment in U373 cells significantly inhibited the colony formation capacity on the cells. It was also determined that increasing doses of avanafil treatment in U373 cells significantly suppressed the colonization capacity of the cells. As a result of the analyses, it was found that the combination of 30 nM and 500 nM paclitaxel, with increasing doses of avanafil, showed a synergistic effect on the cells and inhibited their colony formation capacity more compared to mono treatments in Figs. 3, 4 and 5.

Determination of the Effect of Avanafil and Paclitaxel Combination Treatments on Cancer Cell Migration

To determine the role of avanafil and paclitaxel combination treatments on in vitro cancer cell migration, U373 cells were cultivated, and cell confluency was monitored to be around 90%. Then, a straight line was created with a sterile 100 µL pipette tip. After PBS washes, control, avanafil 31 µg/mL, paclitaxel 1.5 µg/mL, and combination (31 µg/mL + 1.5 µg/mL) groups were formed for U373 and 6-, 12- and 24-hours microscope analyses were performed. Then, each group was normalized to the 0th-hour values. While the 0th-hour and 24th-hour wound patency rate of U373 control cells was determined as 20.1%, the 0th-hour and 24th-hour wound patency rate of avanafil was determined as 60.8% and the 0th-hour and 24th-hour wound patency rate of paclitaxel was determined as 81.1%. The wound patency rate of the combination treatment at 0 and 24 h was determined as 93.9% in Fig. 6. The findings suggest that the combined treatment has a lower wound closure rate compared to mono treatments and thus inhibits the migration on cells.

Determination of the Effects of Avanafil and Paclitaxel Combination Treatments on DNA Damage and Apoptotic Proteins in U373 Cells

In Western blot analysis, 1×10^6 U373 cells were seeded into 6 cm culture dishes. The next day, U373 cells were treated with IC_{50} avanafil (31 µM), IC_{50} paclitaxel (1.5 µM), and the combination of IC_{50} avanafil + IC_{50} paclitaxel for 24 h. Following treatment, cells were collected by trypsinization, and total protein isolation was performed. Protein samples of equal amounts, the concentration of which was determined by Bradford analysis, were run on SDS-PAGE gel, moved to PVDF membrane, incubated with the relevant primary and secondary antibodies, and finally enzymatic HRP activity was transferred to x-ray film and p53, Bax, Bcl-2, Cas-3, Cas-9, and cPARP protein expression profiles were analyzed. When p53 protein expression was first examined in Western blot analysis, it showed a significant increase in U373 cells in all groups. Upon examining the expression of the pro-apoptotic Bax protein, it was determined that the IC_{50} of avanafil and combination groups in U373 cells was significantly decreased compared to the control, whereas the IC_{50} of paclitaxel expression showed an increase. Anti-apoptotic Bcl-2 protein expression was observed to increase significantly with the combination treatment in U373 cells compared to the control in Fig. 7. Cas-3 protein expression, one of the apoptotic markers, was found to be significantly decreased in all combination treatment groups compared to the control in U373 cells. Expression of Cas-9 protein, another apoptotic marker, increased significantly in U373 cells in all groups. It was determined that c-PARP expression, also known as a DNA damage marker, was significantly increased in U373 cells compared to the control in Fig. 8.

In the report published by the International Agency for Research on Cancer in 2020, it was reported that approximately 19 million people were diagnosed with cancer [50]. This report once again reveals that serious steps need to be taken in cancer treatments. Although successful results have been achieved with clinical studies, long-term success is limited due to treatments' serious side effects and existing or acquired drug resistance [51, 52]. The success of these studies in clinical cancer treatment emphasizes the importance

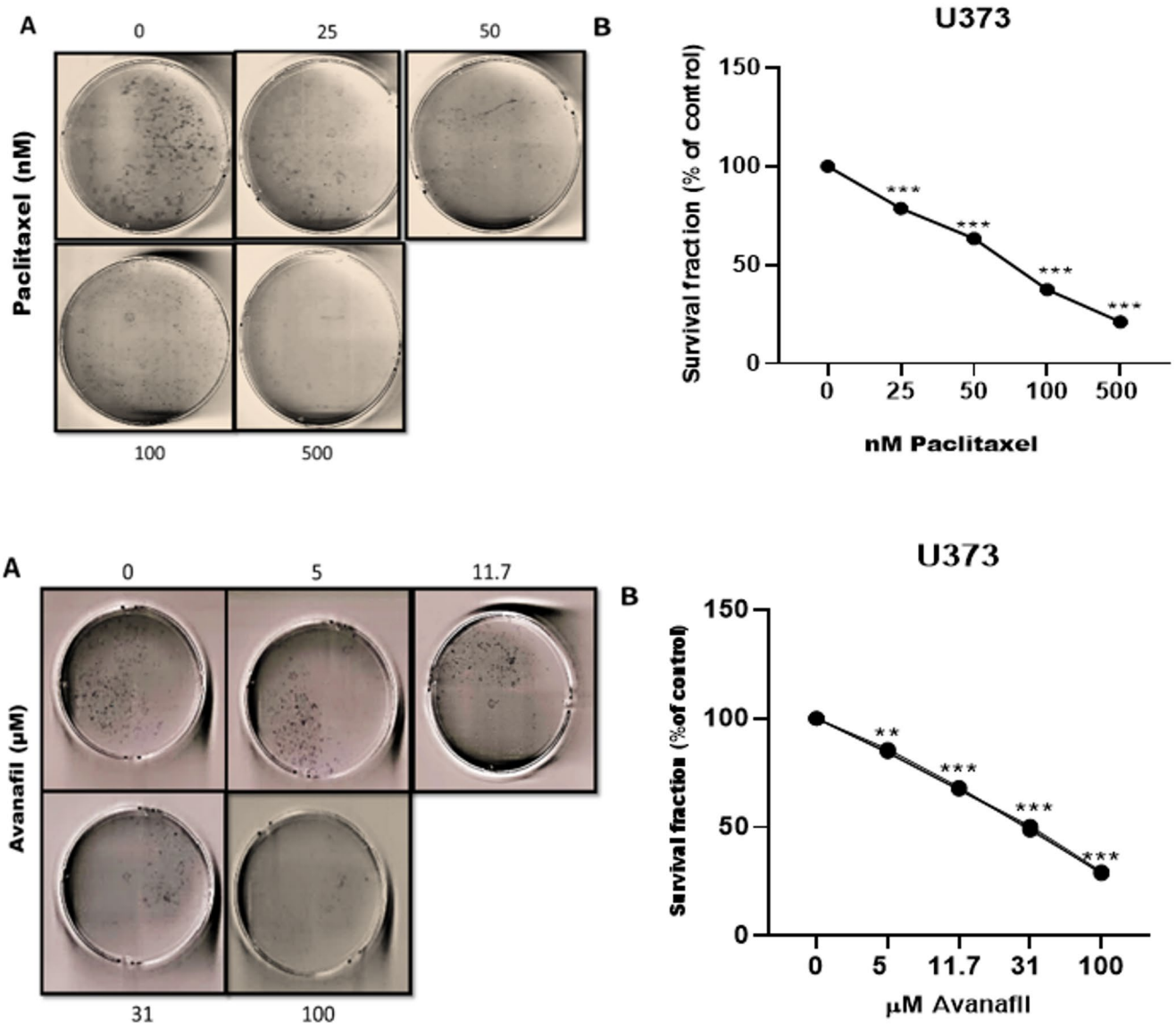

Fig. 3 Effect of Avanafil and Paclitaxel treatments on colony survival in U373 cells (**A**) U373 (5, 11.7, 31, 100 µg/mL) cells were seeded in 6 cm culture dishes and treated with increasing doses of avanafil for 24 h. (**B**) Graph showing the percentage of colonies formed compared to the control group. Effect of Avanafil and Paclitaxel treatments on colony survival in U373 cells (**A**) U373 (25, 50, 100, 500 ng/mL) cells were seeded in 6 cm culture dishes and then treated with increasing doses of paclitaxel for 24 h. (**B**) Graph showing the percentage of colonies formed compared to the control group. *$p<0.05$ compared to control, **$p<0.01$; ***$p<0.001$ compared to control

of pre-clinical cancer treatment approaches [53]. In recent years, studies have focused on the potential of cancer cells to be biomarkers or pharmacological targets in cancer treatment by revealing their genomic, proteomic, transcriptomic, and epigenetic profiles [54–56]. Malignant glioma is the most common intracranial primary brain tumour of the central nervous system in adults. After optimal treatment, the 5-year survival rate of glioma due to invasion, metastasis, and poor prognosis is below 6% [57]. Glioblastoma is an aggressive malignant brain tumour known to occur more commonly in adults [58].

The World Health Organization examines glioblastomas in four stages. In phases I and II, there is an advanced morphology that can be distinguished from normal tissues, while in phases III and IV, there is an increased malignancy that cannot be distinguished from normal tissues. The density status of the cells, nuclear disorders, mitotic processes of the cells, and their proliferation tendency are considered in defining the progression of glioblastoma [59]. Glioblastoma is treated with surgery, radiation, and chemotherapy. Regrettably, treatment methods are not sufficient, and it is stated that cancer cells become resistant to drugs, especially in drug-based treatments such as chemotherapy. This limits

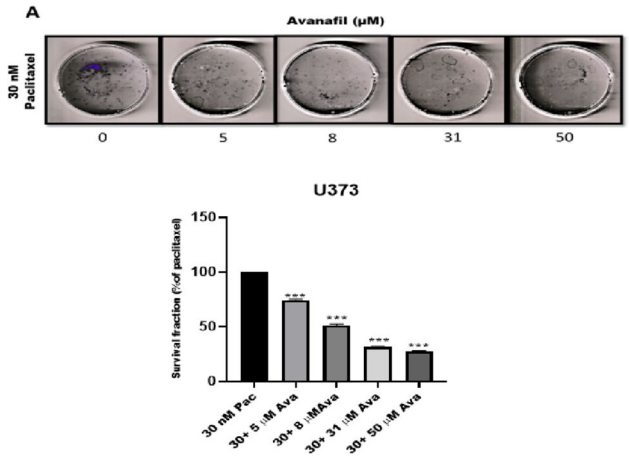

Fig. 4 Effect of Avanafil and Paclitaxel combination treatments on colony survival in U373 and U87 cells (A) U373 and U87 cells were seeded in 6 cm culture dishes, paclitaxel 30 ng/mL and 500 ng/mL were kept constant for 24 h and increasing doses (5, 8, 31, 50 μg/mL) and (3. 5, 10, 32, 50 μg/mL) avanafil treatment. Graph showing the percentage of colonies formed compared to the control group. *$p<0.05$ compared to control, **$p<0.01$, ***$p<0.001$ compared to control

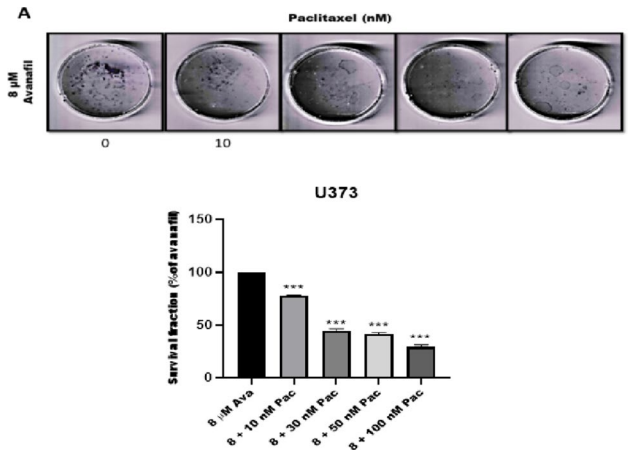

Fig. 5 Effect of Avanafil and Paclitaxel combination treatments on colony survival in U373 cells (**A**) U373 cells were seeded in 6 cm culture dishes and treated with increasing doses (10, 30, 50, 100 ng/mL) of paclitaxel while keeping 8 μg/mL and 10 μg/mL avanafil constant for 24 h. Graph showing the percentage of colonies formed compared to the control group. *$p<0.05$; compared to control, ** $p<0.01$; *** $p<0.001$ compared to control

the success rate, especially in cancers with limited treatment methods such as glioblastoma [60]. In this study, the effectiveness of a new combined treatment model, an alternative to the combined chemotherapy regimen currently used in the treatment of brain tumours, was investigated. Combination treatment with the PDE5 inhibitor avanafil and chemotherapeutic paclitaxel was performed using the brain tumour cell line Glioma (U373). The cytotoxic effect of the relevant combination on cells, DNA damage, apoptosis, and its roles in cell biology were revealed using a brain tumour cell line in this study. Paclitaxel is known as the first approved herbal-derived chemotherapeutic drug with a high mechanism of action. It can stop the division of cancer cells by inhibiting the cell cycle [61]. Paclitaxel phosphorylates Bcl-2 family members through several gene products and signaling molecules to induce apoptosis. It acts in the induction of apoptosis by decreasing the gene expression of antiapoptotic proteins and increasing the gene expression of pro-apoptotic proteins. The previous studies reported that Bcl-2 family members are inhibited by phosphorylation and phosphorylation of Bcl-2 causes the cell to undergo apoptosis [62]. Although paclitaxel is a successful anticancer drug, the variable response of cancer patients to the drug and the drug resistance limit clinical success. For this reason, attempts are being made to increase the success rate with possible combined treatments with various therapeutic agents. Avanafil is a PDE inhibitor and used in the treatment of erectile dysfunction [22]. PDE5 is an enzyme involved in the degradation reactions of cGMP [25]. In MTT analysis, The IC_{25} value of avanafil in U373 cells was determined as 11.7 μg/mL and the IC_{50} value was determined as 31 μg/mL. The paclitaxel IC_{25} value was determined as 100 ng/mL, and the IC_{50} value was determined as 1.5 μg/mL in U373 cells. Nacoulma et al. (2013) found the 72-hour paclitaxel IC_{50} value as 4.5 μg/mL in U373 cells in their study, which supports our results when the treatment duration is considered [63].

Colony survival is an in vitro analysis that involves the transformation of a single cell into a colony of at least fifty cells. Colony survival analysis is widely used to determine the effectiveness of cytotoxic agents on cells [64]. In our study, in which the colony formation capacities of the cells were measured after paclitaxel and avanafil treatments were applied to the U373 cell line. Colony formation of cells was determined under a microscope for approximately 12–14 days. The colony formation capacities of U373 cells were compared with the control groups. Our results revealed that increasing doses of paclitaxel suppressed the clonogenic capacity of U373 cells in a statistically significant way, and only 20.4% of the cells were able to form colonies after the highest dose of 500 nM paclitaxel treatment. Similarly, in the clonogenic assay performed with increasing doses of avanafil, the colony formation abilities of the cells were significantly suppressed depending on the dose. In 100 μM avanafil treatment, the colony formation percentage of the cells was determined as 29%.

As a result, paclitaxel and avanafil mono treatments suppressed the colony formation abilities in U373 cells in a statistically significant way, depending on the dose. In the colony survival analyses, we conducted to investigate the cytotoxicity that may occur because of the combination of paclitaxel and avanafil, avanafil and paclitaxel mono treatments were taken into consideration. In U373 cells, the

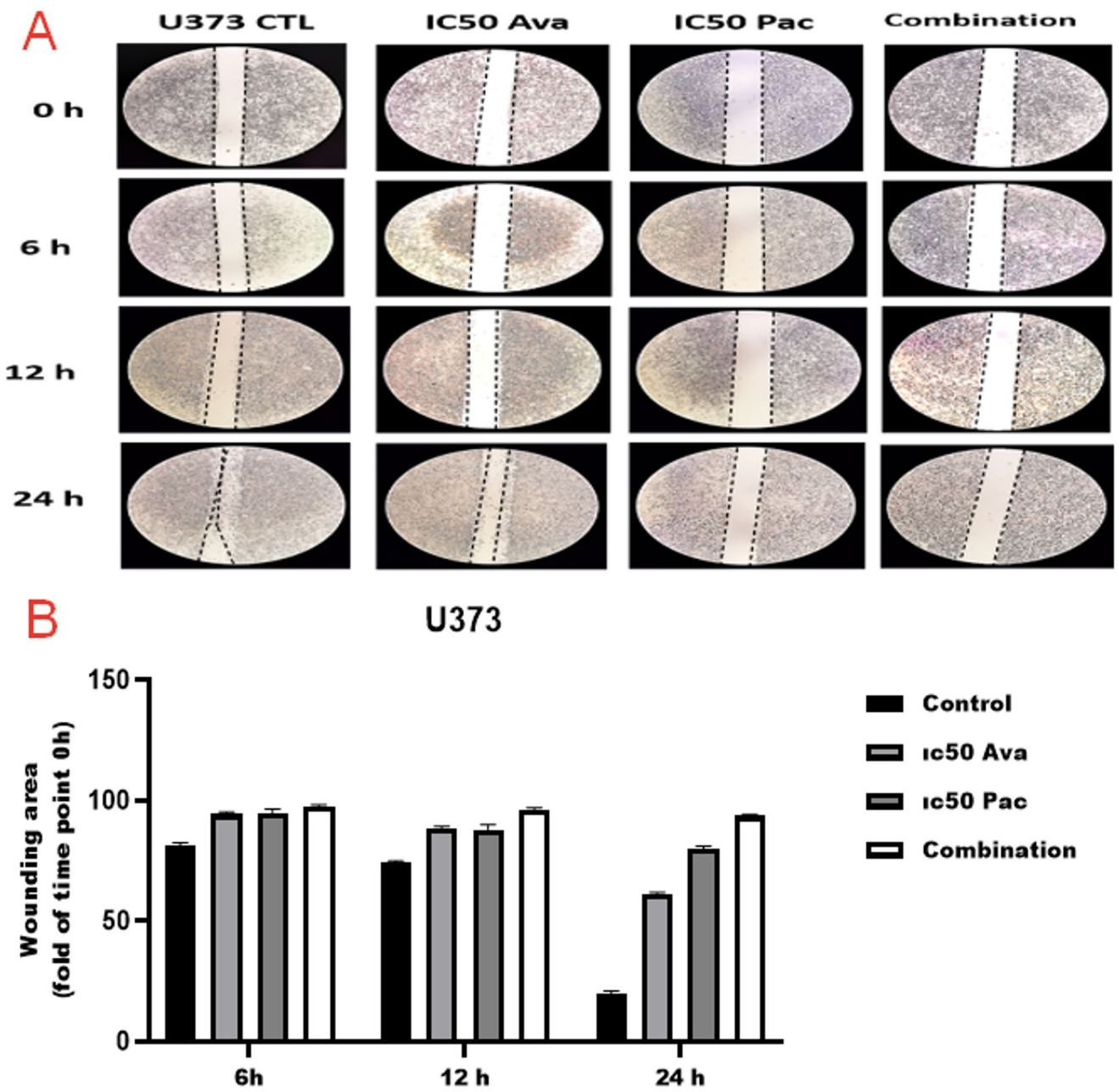

Fig. 6 (**A**, **B**) Effect of avanafil and paclitaxel combination treatments on cancer cell migration in vitro

paclitaxel dose was kept constant at 30 nM, and increasing doses of avanafil (5, 8, 31, 50 µM) treatment were applied. Likewise, the avanafil dose was kept constant at 8 µM, and increasing doses of paclitaxel (10, 30, 50, 100 µM) treatment were applied. Keeping the paclitaxel dose constant and increasing doses of avanafil seriously suppressed the colony formation percentages of the cells. Similarly, in the group where avanafil was kept constant, the colony formation potential of increasing doses of paclitaxel treatment on cells decreased significantly. It was determined that paclitaxel and avanafil combined treatments had a synergistic effect on U373 cells. The effect of avanafil and paclitaxel combination on U373 cancer cell migration in vitro was examined. Wound healing assay is a technique in which the healing process of a wound opened to the cell is followed by cellular migration under in vitro conditions [65].

In our study, paclitaxel (1.5 µg/mL) and avanafil (31 µg/mL) IC_{50} and combination doses were used for U373. Each group was normalized to 0th-hour values. As a result of 24-hour treatment, in U373 cells, the wound opening rate of the control group at 0 h and 24 h was 20.1%, the wound opening rate of avanafil at 0 h and 24 h was 60.8%, the

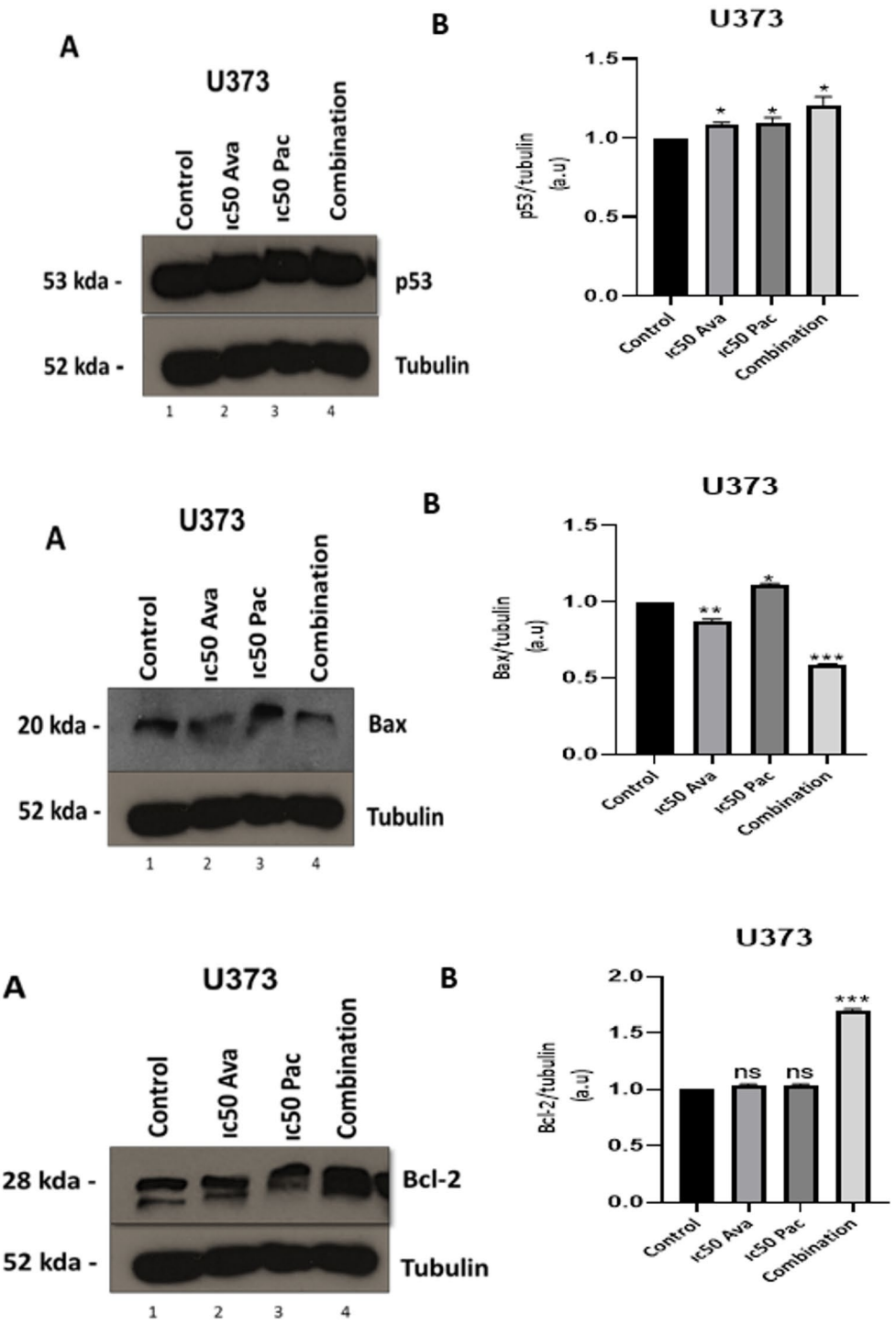

Fig. 7 Effect of Avanafil and Paclitaxel combination treatments on DNA damage and apoptotic proteins in U373 cells (**A**) (**B**) Densitometric analysis of the Western blot results obtained was performed using Image-J programme. *$p<0.05$; compared with control, **$p<0.01$; compared with control, ***$p<0.001$; compared with control, ****$p<0.0001$

wound opening rate of paclitaxel at 0 h and 24 h was 81.1%, and the wound opening rate of the combination treatment at 0 h and 24 h was 93.9%. It was concluded that the wound closure rate of the combination treatment was lower than the mono treatments and thus prevented migration on the cells more. To further verify whether there was a possible association between decreased cell migration and apoptosis or other forms of cell death, Western blot analysis was carried out on the aforementioned treatment groups. Although it was possible to observe a phenotypic expression regarding impaired migration using the wound healing assay, it was possible to make a molecular assessment for apoptosis using Western blot. Notwithstanding impaired migration observed in the wound healing assay, levels of pro-apoptotic proteins such as Bax and Caspase-3 were shown to be decreased; on the contrary, anti-apoptotic protein Bcl-2 was increased

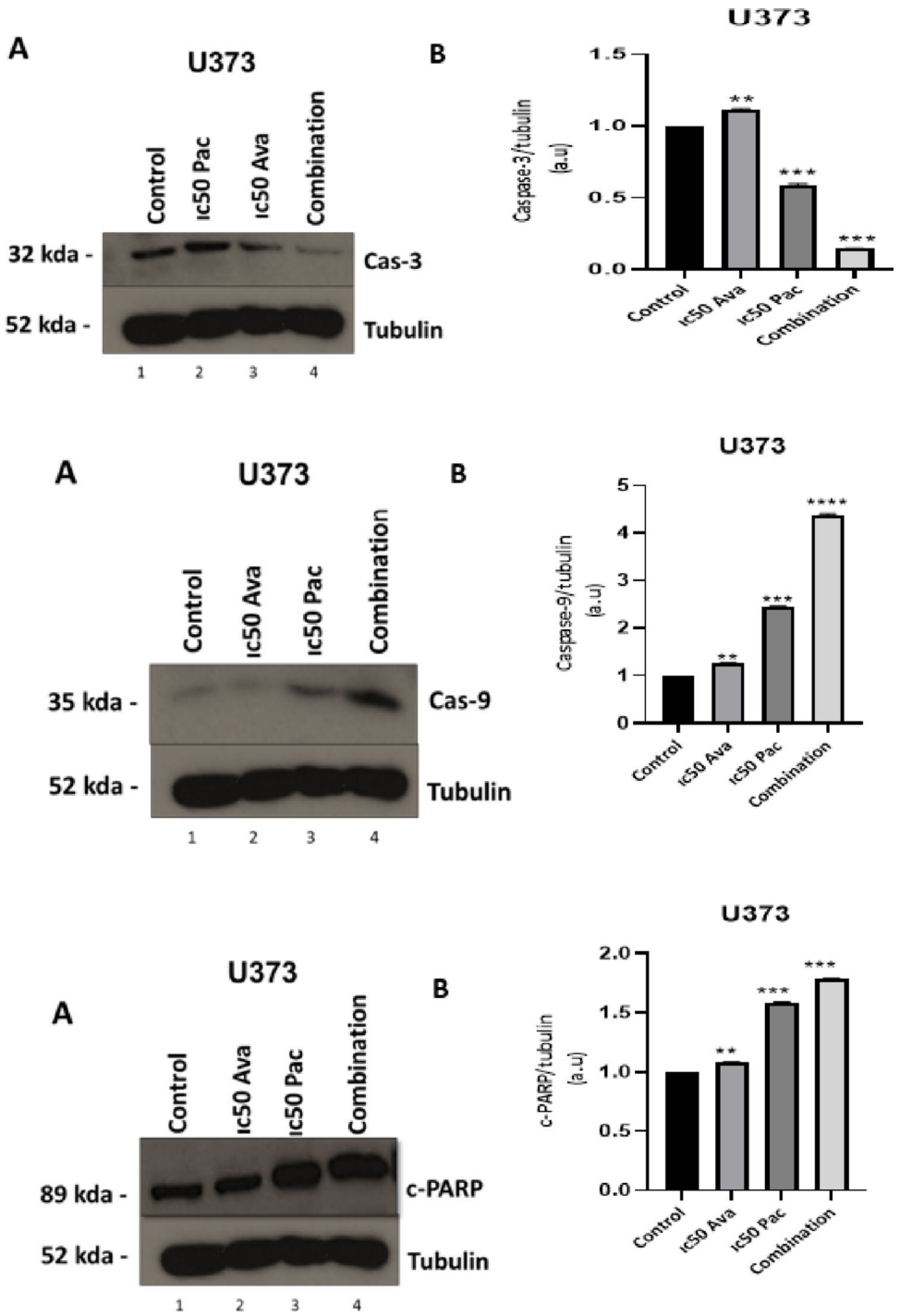

Fig. 8 Effect of Avanafil and Paclitaxel combination treatments on DNA damage and apoptotic proteins in U373 cells (**A**) (**B**) Densitometric analysis of the Western blot results obtained was performed using Image-J programme. *$p<0.05$; compared with control, **$p<0.01$; compared with control, ***$p<0.001$; compared with control, ****$p<0.0001$

in combination. Such apparent inconsistencies indicate that although impaired migration observed in the wound healing assay may not be attributed to apoptosis by a strict definition, it may rather be attributed to some alternative form of apoptosis. Our results revealed that avanafil and paclitaxel treatment significantly increased the cytotoxic effect in U373 cells. The expression levels of p53, Bax, Bcl2, Cas-3, Cas9, and cPARP biological indicators were compared in Western blot analyses performed to monitor programmed cell death (apoptosis) and DNA damage in cells exposed to avanafil and paclitaxel combination treatment. p53 is one of the tumour suppressor proteins that is involved in various cellular pathways. It also acts an essential role, especially in the process of cell cycle arrest and apoptotic activation. When p53 protein expression was first examined in Western blot analysis in U373 cells, a significant increase was determined in all groups. Considering that the increase in p53 may result from damage in DNA, the observed increase

in p53 in individual and combination treatments of avanafil and paclitaxel compared to the control group may be due to damage in DNA [66, 67]. The B-cell lymphoma 2 (B-cell lymphoma 2; BCL-2) protein family has a role in regulating the apoptosis pathway and consists of more than 20 members. Anti-apoptotic proteins consist of members such as BCL-2, BCL-XL, and MCL-1. Anti-apoptotic proteins support cell survival by preventing cells from entering the apoptosis mechanism. Pro-apoptotic proteins (BAX, BAD, BID) support the programmed elimination of cells by promoting apoptosis [68].

When looking at pro-apoptotic Bax protein expression, it was found that IC_{50} of avanafil and combination groups decreased significantly compared to the control, while IC_{50} of paclitaxel expression increased. Anti-apoptotic Bcl-2 protein expression was observed to be significantly increased in U373 cells with the combination treatment compared to the control. It was found that Cas-3 protein expression, one of the apoptotic markers, was significantly reduced in the combination treatment group compared to the control in U373 cells. An examination of the expression levels of Cas-9 protein, another apoptotic marker, revealed a significant increase in U373 cells across all treatment groups. It was determined that the expression of c-PARP, also known as a DNA damage marker, was significantly increased in U373 compared to the control. The decrease in pro-apoptotic proteins and the increase in anti-apoptotic proteins suggest that avanafil and paclitaxel combination treatment may have activated other cellular mechanisms without causing apoptosis in U373 cells. Considering the cytotoxic and apoptosis-inducing effects of paclitaxel [69]. it is proposed that the combination with avanafil reduces the apoptotic effect, leading to toxicity through alternative cellular death pathways.

Theoretical results

Concepts such as the ΔE energy gap, E_{HOMO}, E_{LUMO}, chemical hardness, softness, electronegativity, and chemical potential are very important for understanding the electronic structure and chemical properties of molecules. These are the essential parameters used in assessing the stability and reactivity of chemicals. The energy gap, symbolized as ΔE, quantifies the difference in energy levels between the highest occupied molecular orbital (HOMO) and the lowest unoccupied molecular orbital (LUMO) of a molecule, as shown in reference [70]. Grasping the electrical stability and reactivity of a molecule requires a comprehensive understanding of this value, which is a fundamental prerequisite. A minimal ΔE value indicates heightened molecular reactivity, while a substantial ΔE value implies a more stable molecular structure [71]. In the context of molecular orbital energy, the abbreviations E_{HOMO} and E_{LUMO} denote the energy of the highest occupied molecular orbital and the lowest unoccupied molecular orbital, respectively. The ability of a molecule to donate electrons, referred to as nucleophilic behavior, is dictated by the HOMO, whereas the ability of a molecule to accept electrons, known as electrophilic behavior, is governed by the LUMO [72]. Grasping the mechanics of electron transport in chemical processes requires a comprehensive understanding of the energy differential between the HOMO and LUMO states. The resistance of a molecule to alteration due to external factors is termed its chemical hardness. Molecules that exhibit greater hardness possess a more stable structure and a reduced amount of reactivity. The chemical softness of a molecule is a metric of its reactivity, with soft molecules being more susceptible to changes in their chemical makeup [71]. An grasp of the acid-base properties of molecules and the capacity to predict chemical bond formation may be acquired via the use of hardness and softness concepts. Electronegativity is a crucial parameter for understanding the polarity of chemical bonds. It is a phrase that denotes the tendency of an atom or molecule to attract bonding electrons. Molecules with elevated electronegativity possess a superior ability to attract electrons and exhibit electrophilic characteristics during chemical reactions. As stated in, chemical potential quantifies the energy change inside a molecule and illustrates the system's response to fluctuations in electron density [72]. This value is a crucial indicator in the analysis of reaction energy and molecular stability. Collectively, these words provide a comprehensive framework for understanding a molecule's electrical structure, chemical reactivity, and stability. The assessment of the energy levels of the HOMO and LUMO states, together with ΔE, serves as a very effective tool for forecasting molecular reactivity [73]. In comprehending molecular behavior in reaction to external influences, qualities like chemical hardness, softness, and electronegativity are crucial. A comprehensive enumeration of all parameters is provided in Table 1; Fig. 9.

The ionization energy and electron affinity of a molecule are associated with the energy levels of the HOMO (highest occupied molecular orbital) and LUMO (lowest unoccupied molecular orbital), as Koopman's theorem [74], a significant principle in molecular orbital theory. According to the concept, the energy of the HOMO corresponds to the ionization energy of the molecule, while the energy of the LUMO reflects the electron affinity of the molecule. This approach is a powerful tool for precisely predicting the electrical properties and reactivity of molecules [75]. The results, however, are just an approximation since the theory neglects electron-electron interactions. The findings may need further, more complex calculations. To enhance comprehension of acid-base chemistry, the Hard and Soft Acid-Base concept (HSAB) was developed [76]. This notion posits that

Table 1 The calculated quantum chemical parameters of molecules

	E_{HOMO}	E_{LUMO}	I	A	ΔE	η	μ	χ	PA	ω	ε	dipol	Energy
B3LYP/6–31 g LEVEL													
A	−5.3161	−1.5745	5.3161	1.5745	3.7416	1.8708	0.5345	3.4453	−3.4453	3.1724	0.3152	6.058	−53344.359
P	−6.0252	−2.1968	6.0252	2.1968	3.8284	1.9142	0.5224	4.1110	−4.1110	4.4144	0.2265	14.356	−72420.111
A-P	−5.4007	−1.5780	5.4007	1.5780	3.8227	1.9113	0.5232	3.4893	−3.4893	3.1851	0.3140	2.708	−125762.886
HF/6–31 g LEVEL													
A	−5.6078	−1.8773	5.6078	1.8773	3.7304	1.8652	0.5361	3.7425	−3.7425	3.7547	0.2663	7.196	−53346.030
P	−6.4728	−2.6428	6.4728	2.6428	3.8300	1.9150	0.5222	4.5578	−4.5578	5.4239	0.1844	12.510	−72423.270
A-P	−8.2223	2.0401	8.2223	−2.0401	10.2623	5.1312	0.1949	3.0911	−3.0911	0.9311	1.0740	3.016	−125040.809
M062X/6–31 g LEVEL													
A	−5.6192	−1.7222	5.6192	1.7222	3.8970	1.9485	0.5132	3.6707	−3.6707	3.4576	0.2892	7.087	−53359.993
P	−6.1787	−2.1777	6.1787	2.1777	4.0009	2.0005	0.4999	4.1782	−4.1782	4.3633	0.2292	10.593	−72445.846
A-P	−6.7724	−0.6449	6.7724	0.6449	6.1275	3.0638	0.3264	3.7087	−3.7087	2.2447	0.4455	2.679	−125719.466

A: Avanafil, P: Paclitaxel, A-P: Avanafil and Paclitaxel combinations

robust interactions occur between hard acids and hard bases, whereas powerful interactions arise between soft acids and soft bases using hard acids. Conversely, the term "soft" denotes attributes such as low polarizability, large size, and high polarizability, and "hard" is defined by qualities like high ionization energy, small size, and low polarizability. The Maximum Hardness Principle (MHP) posits that chemical systems prefer to form structures exhibiting the maximum attainable hardness. This notion posits that a system tends to adopt a structure characterized by increasing rigidity. The enhanced structure is less reactive and more stable because to its greater hardness. This idea functions as an essential framework for predicting molecular stability and the reactions involved in chemical processes [77]. The maximum hardness notion is often used in the generation of reactive intermediates and the evaluation of transition states. A thorough understanding of molecular reactivity and bonding characteristics may be achieved via these three essential concepts, which provide both theoretical and practical foundations. Koopman's theorem is used to investigate electron transport mechanisms. The HSAB concept is used to elucidate the characteristics of acid-base interactions. Moreover, PMH significantly contributes to the prediction of molecular stability [78]. Utilizing these approaches in combination enables a comprehensive understanding of chemical system behavior.

Calculations were made using the Gaussian package program for 3 different molecules consisting of Avanafil, Paclitaxel, and Avanafil and Paclitaxel combinations. In the calculations made at all three levels, when the HOMO energy numerical value was compared, it was seen that the Avanafil molecule had higher activity than the other molecules. In addition, according to the LUMO energy numerical value of the molecules, it was seen that the Paclitaxel molecule had higher activity than the other molecules at all three levels. According to the energy gap energy numerical value of the molecules, it was seen that the Avanafil molecule had higher activity than the other molecules. Finally, when the molecules were compared according to the electronegativity energy numerical value, it was seen that the Avanafil and Paclitaxel combination had higher activity at the HF level, and the Avanafil molecule had higher activity than the others at the B3LYP and M062X levels.

Each molecule has distinct energy levels and numerical values for various characteristics in Table 1. New and more effective molecular groups were synthesized by the combination of these compounds, although their thermodynamic properties did not provide any signs of spontaneous production in Table 2. The numerical values for each molecule were also provided in Table 3. ΔE, ΔH, and ΔG were computed using the following equations:

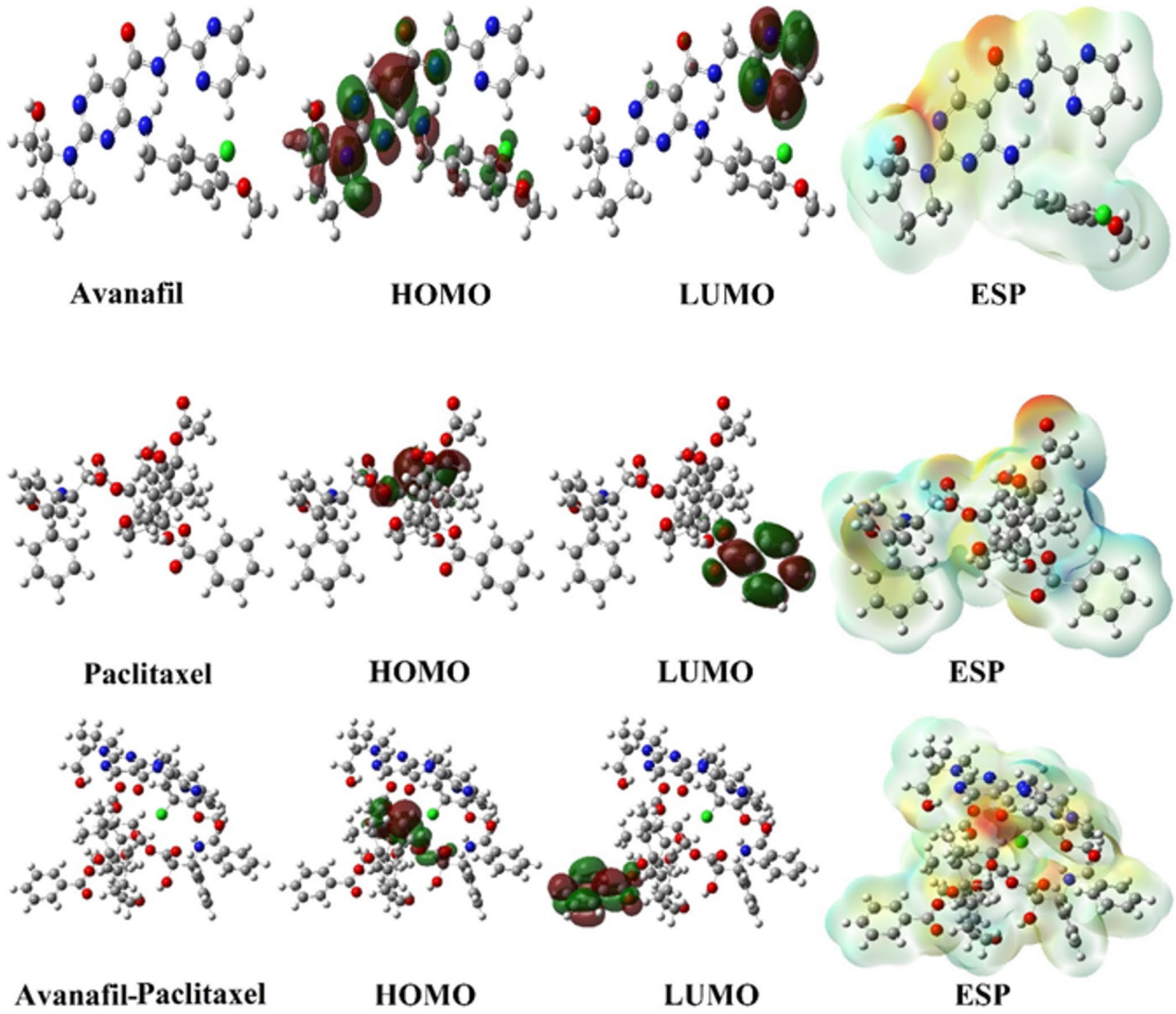

Fig. 9 Representations of optimize structure, HOMO, LUMO, and ESP of molecules

Table 2 Numerical value of the molecules' physicochemical parameters

		E	H	G
B3LYP	A	−53341.655	−53341.629	−53344.360
	P	−72416.285	−72416.260	−72420.112
	A-P	−125758.776	−125758.750	−125762.886
HF	A	−53065.694	−53065.668	−53068.292
	P	−71968.541	−71968.515	−71972.212
	A-P	−125035.368	−125035.342	−125040.809
M062X	A	−53324.804	−53324.778	−53327.396
	P	−72389.032	−72389.006	−72392.726
	A-P	−125715.289	−125715.263	−125719.466

A: Avanafil, P: Paclitaxel, A-P: Avanafil and Paclitaxel combinations

Table 3 Numerical value of the molecules' physicochemical parameters

	B3LYP	HF	M062X
ΔG	1.58464	−0.30491	0.65634
ΔH	−0.86138	−1.15905	−1.47865
ΔE	−0.83567	−1.13336	−1.45296

$$\Delta E = \sum E_{complex} - \sum E_{molecule}$$

$$\Delta H = \sum E_{complex} - \sum E_{molecule}$$

$$\Delta G = \sum E_{complex} - \sum E_{molecule}$$

Energy E, including electronic and thermal energies, is a crucial thermodynamic parameter that signifies the

aggregate of E0, Evib, Erot, and Etransl energies. Energy H, conversely, represents the aggregate of all forms of energy contained inside the structure. The energy G is determined by subtracting these two previous total energy values [79].

This table shows the comparison of ΔG, ΔH and ΔE values obtained using three different calculation methods (B3LYP, HF and M06X). While ΔG value was found positive in B3LYP and M062X methods (B3LYP: +1.58464, M06X: +0.65634), it was calculated as −0.30491 in HF method. A negative Gibbs free energy indicates that the process under study tends to occur spontaneously, while a positive one indicates that it is not spontaneous [80].

This difference may be due to the change in entropic contributions and electron correlation calculations from method to method. In terms of enthalpy change (ΔH), all three methods give negative values (B3LYP: −0.86138, HF: −1.15905, M062X: −1.47865). This situation reveals the exothermic nature of the relevant interaction or reaction [81]. The M062X method, which gives the lowest (i.e. the most negative) ΔH value, found the binding or reaction energy stronger than the other methods. Electronic energy change (ΔE) values are also negative in all methods, and the HF and M062X methods predict a larger energy gain (more negative value) than B3LYP. This result suggests that the HF and M062X methods predict a more stable or stronger interactive structure than B3LYP. As a result, it is important to verify with experimental data or more advanced calculations to determine which method gives results closer to reality.

Table 4 Numerical values of the docking parameters of molecules against proteins (kcal/mol)

2DME	Avanafil	Paclitaxel	Avanafil and Paclitaxel combinations
Docking Score	−3.69	−4.85	−6.94
Glide ligand efficiency	−0.11	−0.09	−0.08
Glide hbond	−0.57	−0.21	−0.6
Glide evdw	−24.9	−33.41	−42.72
Glide ecoul	−14.1	−12.9	−22.17
Glide emodel	−45.94	−59.86	−74.13
Glide energy	−39.01	−46.31	−64.89
Glide einternal	7.46	7.97	43.24
Glide posenum	282	242	391
6YPE	Avanafil	Paclitaxel	Avanafil and Paclitaxel combinations
Docking Score	-	−6.38	−7.91
Glide ligand efficiency	-	−0.11	−0.09
Glide hbond	-	−0.47	−0.42
Glide evdw	-	−52.64	−69.63
Glide ecoul	-	−10.27	−14.7
Glide emodel	-	−79.26	−116.69
Glide energy	-	−62.91	−84.33
Glide einternal	-	15.94	26.08
Glide posenum	-	82	110

Recent studies demonstrate that the comparison of molecular biological activities has been accelerated and streamlined owing to the widespread application of theoretical research and technology advancements [82]. The identification of the most effective and successful pharmaceuticals prior to experimental testing has been significantly expedited and optimized by the application of calculations [83]. The theoretical calculations resulted in the identification of specific parameters. This approach evaluates the biological activity of molecules about the quantitative values of diverse parameters. The principal factor affecting the activities in question is the interactions between chemicals and specific proteins. These interactions are so widespread that they ultimately impede the proper functioning of the proteins [84]. This is the method by which inhibition transpires. The energy levels of molecules are determined by the interactions between proteins and other molecules. Molecules and protein interactions occur through hydrogen bonds, polar and hydrophobic contacts, π-π interactions, and halogen interactions [85–87]. Molecular interactions are essential for maintaining a state of equilibrium. An exhaustive examination of these chemical interactions demonstrates that molecules and proteins interact with one another in many manners. Table 4 encompasses all factors, whereas Figs. 10, 11, 12, 13 and 14 present all illustrations.

The Glide Ligand Efficiency is the principal metric obtained from molecular docking simulations. Additional complimentary traits exist that are equivalent to these. This numerical depiction demonstrates the effectiveness of the ligand against specific bacterial proteins. The Glide Hbond measurement estimates the quantity of hydrogen bonds established during interactions between proteins and molecules [81]. The Van der Waals interaction number, also known as Glide Evdw [82] serves as a supplementary measure that elucidates the interactions between chemicals and proteins. Furthermore, a metric termed Glide Ecoul quantitatively assesses the Coulomb interactions between proteins and chemicals [83]. The Glide Einternal is a quantitative metric obtained from the synthesis of many elements. This is the definitive parameter obtained from these calculations.

Subsequent to evaluating the biological activities of the compounds against various proteins, ADME/T study was performed to theoretically forecast the effects and interactions of the most active molecules within human metabolism [81]. A range of factors was identified in this theoretical investigation, as illustrated in Table 5.

ADME/T simulations performed with Schrödinger Maestro software are crucial for evaluating the pharmacokinetic

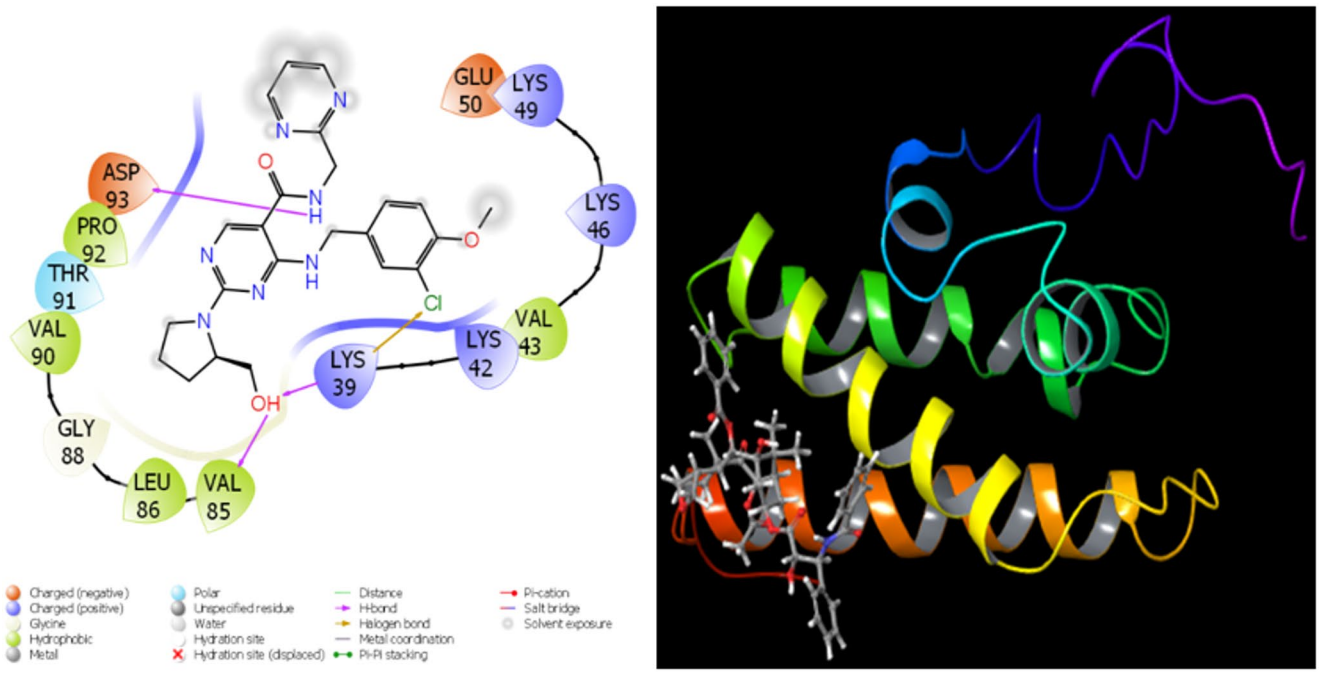

Fig. 10 Presentation interactions of Avanafil with 2DME protein

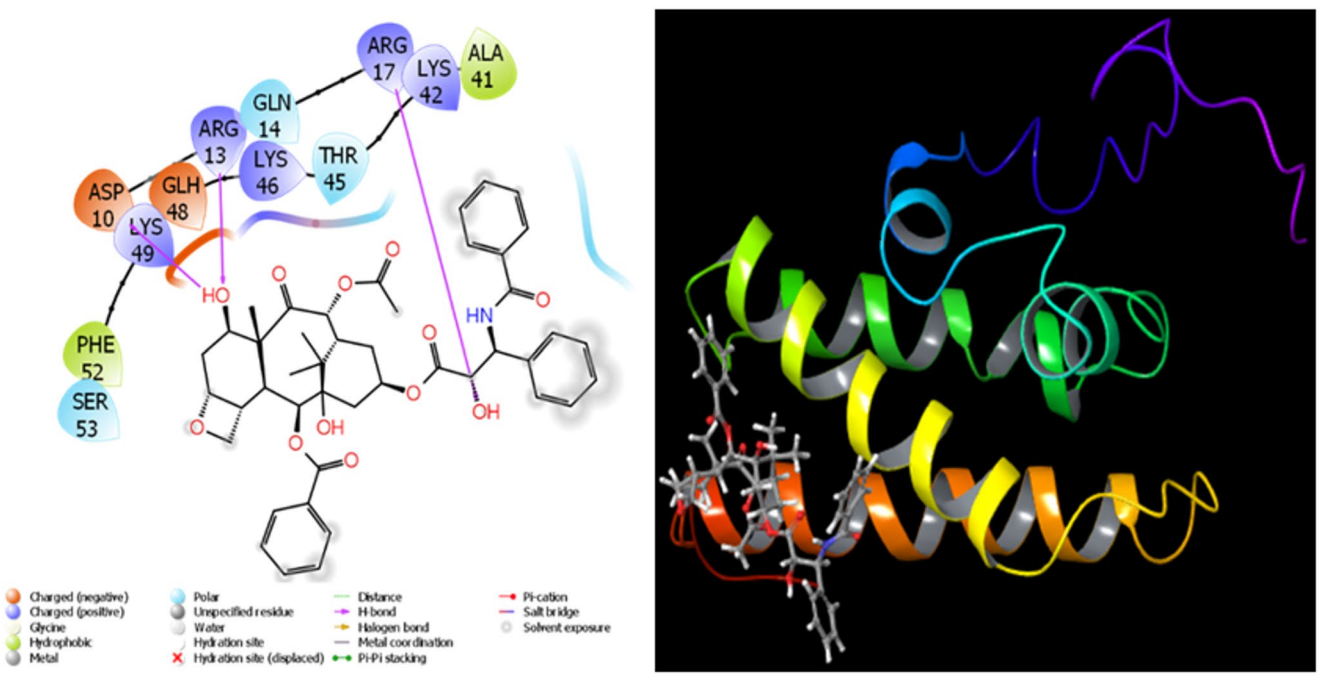

Fig. 11 Presentation interactions of Paclitaxel with 2DME protein

and toxicological properties of substances in drug development [82]. These simulations aid in predicting the behavior of a potential chemical within biological systems. The Schrödinger program provides a comprehensive analysis of ADME/T parameters with the QikProp module. The subsequent parameters are frequently calculated, along by their descriptions. Molecular Weight (MW) signifies the total atomic mass of a molecule. According to Lipinski's "Rule of 5," a medicine candidate is generally deemed successful if its molecular weight is below 500 daltons. LogP (Hydrophobicity or Lipophilicity) measures the octanol/water partition coefficient of a molecule, hence evaluating its lipophilicity. Both low and high LogP values may signify insufficient bioavailability or possible toxicity. The optimal LogP

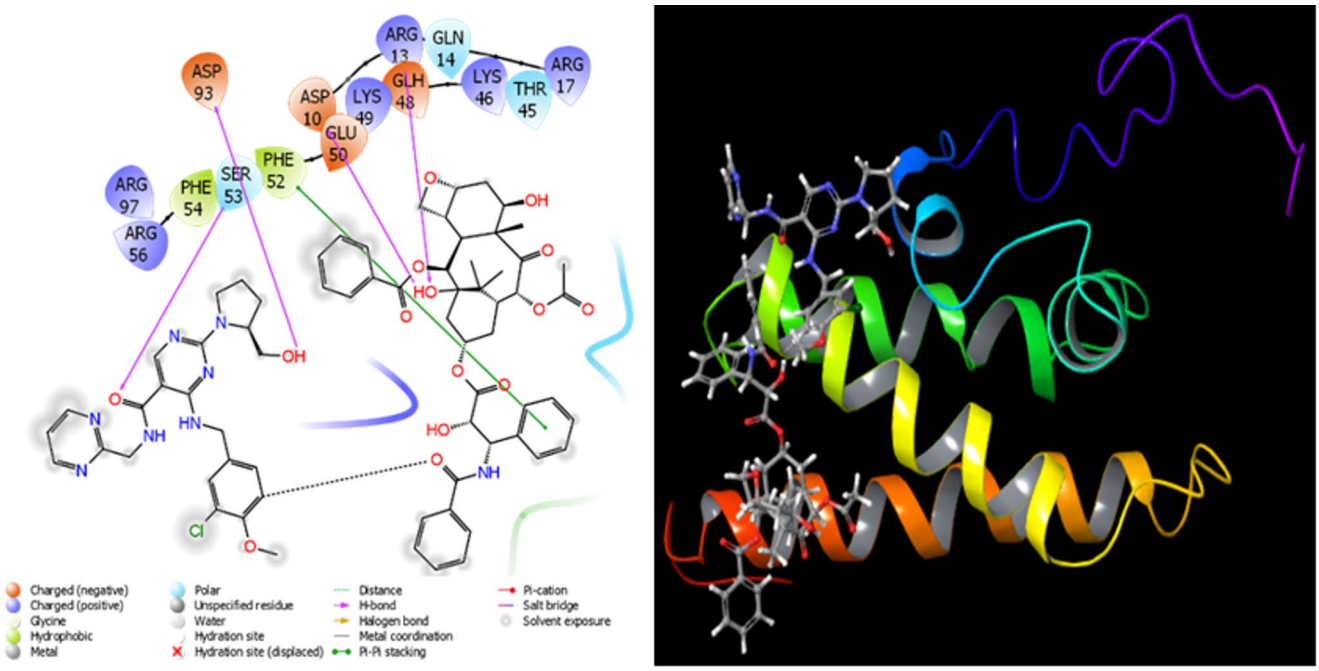

Fig. 12 Presentation interactions of Avanafil and Paclitaxel combinations with 2DME protein

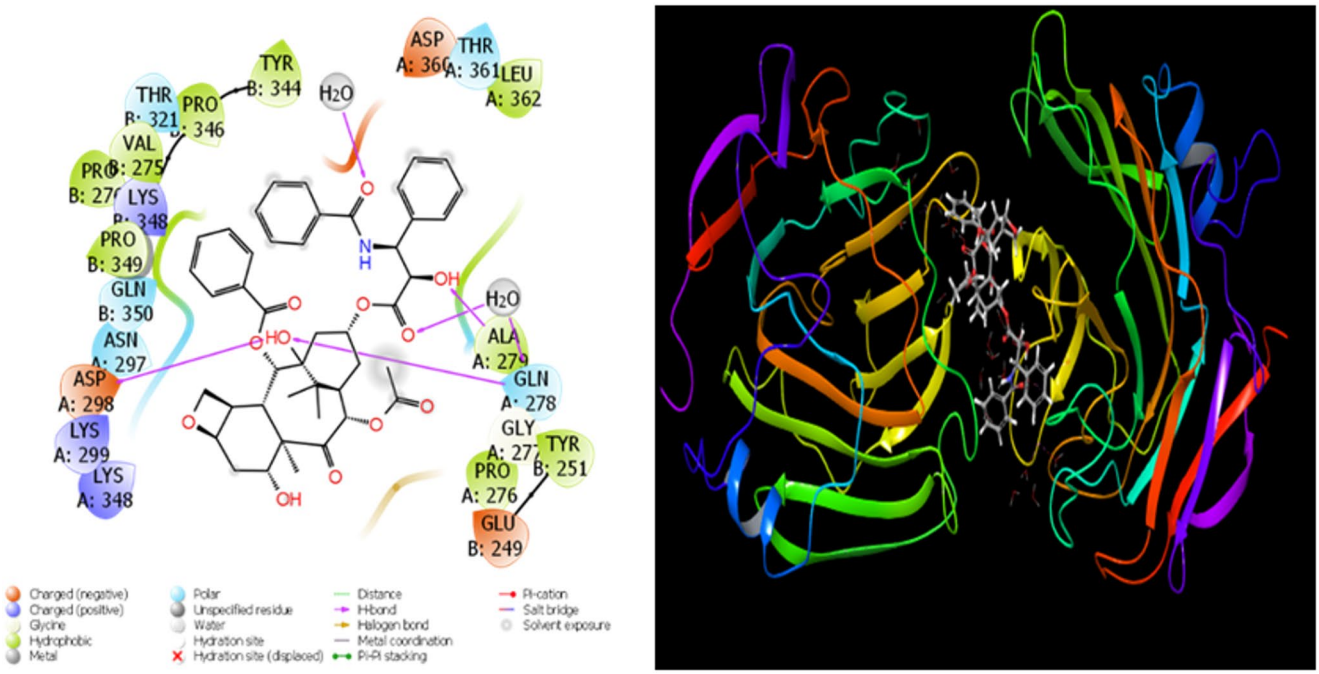

Fig. 13 Presentation interactions of Paclitaxel molecule with 6YPE protein

number generally falls between 0 and 3. Hydrogen Bond Donors and Acceptors (HBD/HBA) refer to the number of functional groups in a molecule that can establish hydrogen bonds. The number of hydrogen bond donors (HBD) and hydrogen bond acceptors (HBA) affects a molecule's solubility and its permeability through biological membranes [83]. In drug-like compounds, it is typically advantageous for the number of hydrogen bond donors (HBD) to be five or less, and for the number of hydrogen bond acceptors (HBA) to be ten or fewer. Total Polar Surface Area (TPSA) refers to the surface area filled by polar functional groups within the molecule. TPSA relates to the solubility of the chemical and its ability to penetrate biological membranes. A TPSA below 140 Å² suggests advantageous bioavailability.

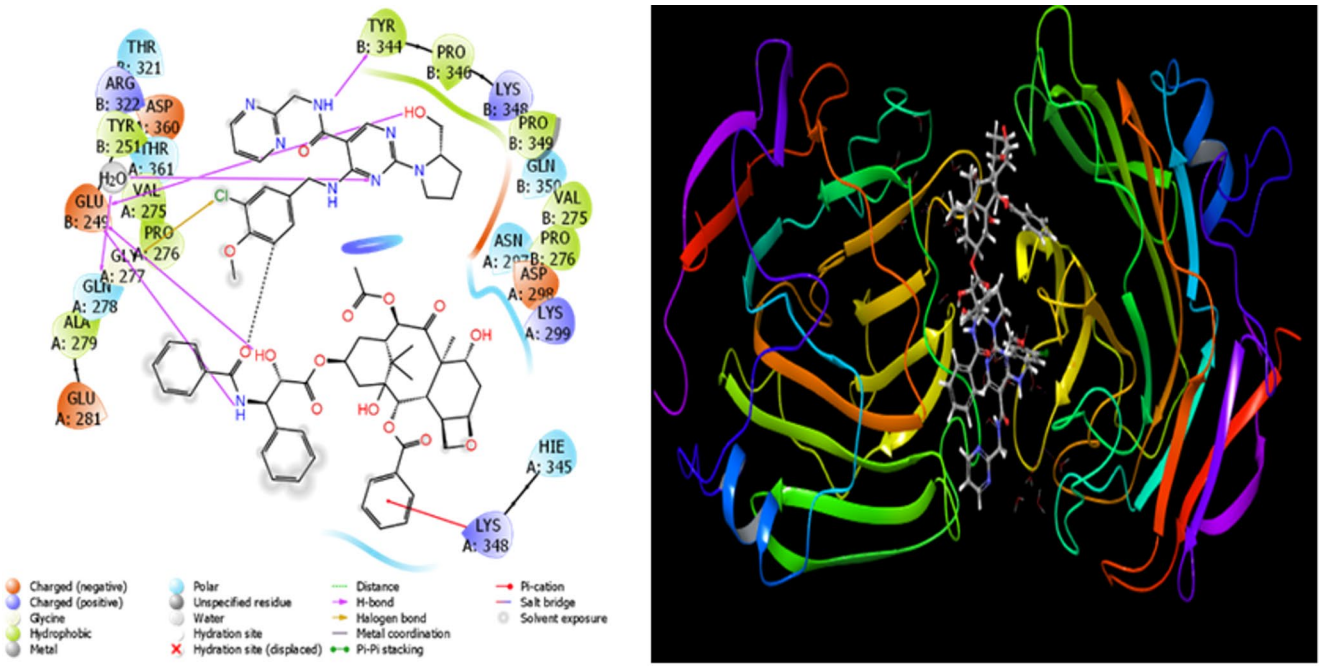

Fig. 14 Presentation interactions of Avanafil and Paclitaxel combinations with 6YPE protein

Aqueous Solubility (LogS) quantifies a molecule's solubility in water. The LogS value affects the bioavailability of the drug candidate and the formulation processes [84].

Molecules with low solubility generally have restricted bioavailability. Plasma Protein Binding (PPB) denotes the fraction of a substance that adheres to plasma proteins. Increased binding to plasma proteins may lower the free concentration of the drug and limit its efficacy. Blood-Brain Barrier Permeability; Signifies the molecule's ability to penetrate the blood-brain barrier. Elevated blood-brain barrier (BBB) permeability is beneficial for pharmaceuticals aimed at central nervous system problems, whereas reduced BBB permeability may decrease toxicity in systemic therapies [85, 86]. Metabolic Stability: Predicts the velocity at which a compound is processed by hepatic enzymes. Improved metabolic stability extends the half-life and therapeutic effectiveness of the drug. Toxicity Predictions (HERG Inhibition, Hepatotoxicity); HERG channel inhibition is evaluated for potential cardiotoxicity. The risk of hepatotoxicity associated with the substance may be evaluated. The Caco-2 cell monolayer assay simulates the translocation of a substance across the human intestinal epithelium. Increased Caco-2 permeability signifies advantageous intestinal absorption. Percent Absorption: Predicts the amount of a chemical that will be absorbed when taken orally. A high absorption rate is an essential attribute of an effective pharmaceutical drug [87, 88]. Lipinski's "Rule of Five" (RO5) is a standard employed to evaluate the pharmacological properties of a compound [89]. These guidelines were formulated to determine the probability that a chemical will have advantageous oral bioavailability. The Rule of Five factors encompass Molecular Weight (MW), LogP, Hydrogen Bond Donors (HBD), and Hydrogen Bond Acceptors (HBA). The "Rule of Three" (RO3) is a standard employed to identify lead compounds in the pharmaceutical development process [90]. This rule highlights the identification of low molecular weight, chemically simpler substances that are subject to more stringent limits than RO5. According to RO3, a molecule must meet specific criteria to be classified as a lead molecule. The Rule of Five includes the criteria of Molecular Weight (MW), LogP, Hydrogen Bond Donors (HBD), Hydrogen Bond Acceptors (HBA), and Rotatable Bonds. All parameters are expected to satisfy the required criteria; hence, the values of these two parameters are forecasted to be zero [91]. It functions as an essential tool for assessing toxicological risks during the medication development process through its calculations. These simulations predict the probability of a suggested chemical causing detrimental effects in biological systems. It assesses numerous toxicity parameters utilizing Schrödinger, QikProp, and additional modules. The initial parameter is HERG Channel Inhibition (Cardiotoxicity); HERG (Human Ether-à-go-go-Related Gene) channels are potassium ion channels that regulate the electrical activity of cardiac myocytes. Another criterion is Blood-Brain Barrier (BBB) Toxicity; chemicals that can penetrate the blood-brain barrier may elicit hazardous effects on the central nervous system. Another metric is the substrate and inhibition of P-glycoprotein (P-gp). P-glycoprotein serves to prevent detrimental accumulation by expelling substances from cells [92].

Table 5 ADME properties of molecules

	Avanafil	Paclitaxel	Avanafil and Paclitaxel combinations	Reference Range
mol_MW	486	784	-	130–725
Dipole (D)	18.1	14.6	-	1.0–12.5.0.5
SASA	729	966	-	300–1000
FOSA	349	319	-	0–750
FISA	113	195	-	7–330
PISA	215	451	-	0–450
WPSA	52.7	0	-	0–175
Volume (A^3)	1397	2044	-	500–2000
DonorHB	3	2	-	0–6
acceptHB	7.0	14.7	-	2.0–20.0
glob (Sphere = 1)	0.8	0.8	-	0.75–0.95
QPpolrz (A^3)	46.0	72.3	-	13.0–70.0
QPlogPC16	14.5	21.7	-	4.0–18.0
QPlogPoct	26.7	37.5	-	8.0–35.0
QPlogPw	13.0	21.2	-	4.0–45.0
QPlogPo/w	4.5	5.0	-	−2.0-6.5
QPlogS	−5.6	−6.2	-	−6.5-0.5
CIQPlogS	−7.3	−9.9	-	−6.5-0.5
QPlogHERG	−5.3	−6.8	-	*
QPPCaco (nm/sec)	833	139	-	**
QPlogBB	−1.0	−2.2	-	−3.0-1.2
QPPMDCK (nm/sec)	789	59	-	**
QPlogKp	−2.0	−2.4	-	Kp in cm/hr
IP (ev)	4.4	9.4	-	7.9–10.5
EA (eV)	2.3	0.8	-	−0.9-1.7
#metab	6	6	-	1–8
QPlogKhsa	0.6	0.7	-	−1.5-1.5
Human Oral Absorption	3	1	-	-
Percent Human Oral Absorption	100	56	-	***
PSA	116	180	-	7–200
RuleOfFive	0	3	-	Maximum is 4
RuleOfThree	0	1	-	Maximum is 3
Jm	0.0	0.0	-	-

Conclusion

The work proved that the co-administration of paclitaxel and avanafil has a synergistic cytocidal and antimigratory effect upon the U373 glioma cell line potentially via apoptotic and non-apoptotic modes. In vitro research indicated the potentiation of DNA damage and the migration impairment in the cells, and results of the docking study and quantum chemistry calculations confirmed the favorable binding patterns with the proteins involved in gliomas. The combination of ADME/T properties could exhibit a spontaneous interaction potential despite certain restrictions.

Acknowledgements The numerical calculations reported in this paper were fully/partially performed at TUBITAK ULAKBIM, High Performance and Grid Computing Center (TRUBA resources). This work was supported by the Scientific Research Project Fund of Sivas Cumhuriyet University (CUBAP) under the project number RGD-020 and by the BAP from Atatürk University (grant number 2022-FKP-11211).

Funding Open access funding provided by the Scientific and Technological Research Council of Türkiye (TÜBİTAK).

Declarations

Conflict of interest The authors declare no conflicts of interest.

Open Access This article is licensed under a Creative Commons Attribution 4.0 International License, which permits use, sharing, adaptation, distribution and reproduction in any medium or format, as long as you give appropriate credit to the original author(s) and the source, provide a link to the Creative Commons licence, and indicate if changes were made. The images or other third party material in this article are included in the article's Creative Commons licence, unless indicated otherwise in a credit line to the material. If material is not included in the article's Creative Commons licence and your intended use is not permitted by statutory regulation or exceeds the permitted use, you will need to obtain permission directly from the copyright holder. To view a copy of this licence, visit http://creativecommons.org/licenses/by/4.0/.

References

1. I. Jovčevska, N. Kočevar, R. Komel, Glioma and glioblastoma-how much do we (not) know? Mol. Clin. Oncol. **1**(6), 935–941 (2013)
2. F. Bray, M. Laversanne, H. Sung, J. Ferlay, R.L. Siegel, I. Soerjomataram, A. Jemal, Global cancer statistics 2022: GLOBOCAN estimates of incidence and mortality worldwide for 36 cancers in 185 countries. Cancer J. Clin. **74**(3), 229–263 (2024)
3. A. Eddhimi, A. Rafik, B. Tüzün, G. Jhaa, K. Yamni, H. Zouihri, Growth, molecular docking, Hirshfeld surface analysis and first-principles investigation on the structural, morphological and mechanical properties of the OIH hybrid: C2H8N4S22+· 2HSO4− under pressure. J. Mol. Struct. **1324**, 140809 (2025)
4. T.T. Lah, M. Novak, B. Breznik, (2020, February). Brain malignancies: Glioblastoma and brain metastases. In *Seminars in cancer biology*. (Vol. 60, 262–273). Academic Press
5. M. Vargo, *Cancer of the Brain, Eye, and Other Parts of the Central Nervous System* (A Concise and Portable Pocket Guide, Cancer Rehabilitation, 2020), pp. 45–67
6. Y. Cheng, R.A. Morshed, B. Auffinger, A.L. Tobias, M.S. Lesniak, Multifunctional nanoparticles for brain tumor imaging and therapy. Adv. Drug Deliv. Rev. **66**, 42–57 (2014)
7. B.H. Menze, A. Jakab, S. Bauer, J. Kalpathy-Cramer, K. Farahani, J. Kirby, Van K. Leemput, The multimodal brain tumor image segmentation benchmark (BRATS). IEEE Trans. Med. Imaging. **34**(10), 1993–2024 (2014)

8. C.D. Arvanitis, G.B. Ferraro, R.K. Jain, The blood–brain barrier and blood–tumour barrier in brain tumours and metastases. Nat. Rev. Cancer. **20**(1), 26–41 (2020)
9. F. Della Ragione, V. Cucciolla, A. Borriello, V. Della Pietra, L. Racioppi, G. Soldati, V. Zappia, Resveratrol arrests the cell division cycle at S/G2 phase transition. Biochem. Biophys. Res. Commun. **250**(1), 53–58 (1998)
10. D. Reichel, B. Sagong, J. Teh, Y. Zhang, S. Wagner, H. Wang, J.M. Perez, Near infrared fluorescent nanoplatform for targeted intraoperative resection and chemotherapeutic treatment of glioblastoma. ACS Nano **14**(7), 8392–8408 (2020)
11. D.N. Louis, A. Perry, P. Wesseling, D.J. Brat, I.A. Cree, D. Figarella-Branger, D.W. Ellison, The 2021 WHO classification of tumors of the central nervous system: a summary. Acta Neuropathol. **142**(1), 11–28 (2021)
12. G.J. Müller, C. Stadelmann, L. Bastholm, F. Elling, H. Lassmann, F.F. Johansen, Ischemia leads to apoptosis—and necrosis-like neuron death in the ischemic rat hippocampus. Brain Pathol. **14**(4), 415–424 (2004)
13. S. Shalini, L. Dorstyn, S. Dawar, S. Kumar, Old, new and emerging functions of caspases. Cell Death Differ. **22**(4), 526–539 (2015)
14. D.S. Ziegler, A.L. Kung, M.W. Kieran, Anti-apoptosis mechanisms in malignant gliomas. J. Clin. Oncol. **26**(3), 493–500 (2008)
15. O. Mukherjee, S. Rakshit, G. Shanmugam, K. Sarkar, Role of chemotherapeutic drugs in immunomodulation of cancer. Curr. Res. Immunol. **4**, 100068 (2023)
16. D. Majumdar, Y. Agrawal, R. Thomas, Z. Ullah, M.K. Santra, S. Das, D. Mishra, Syntheses, characterizations, crystal structures, DFT/TD-DFT, luminescence behaviors and cytotoxic effect of bicompartmental Zn (II)-dicyanamide Schiff base coordination polymers: an approach to apoptosis, autophagy and necrosis type classical cell death. Appl. Organomet. Chem. **34**(1), e5269 (2020)
17. D.G. Kingston, J.P. Snyder, The quest for a simple bioactive analog of paclitaxel as a potential anticancer agent. Acc. Chem. Res. **47**(8), 2682–2691 (2014)
18. L. Zhu, L. Chen, Progress in research on paclitaxel and tumor immunotherapy. Cell. Mol. Biol. Lett. **24**(1), 40 (2019)
19. L. Bui, A. Hendricks, J. Wright, C.J. Chuong, D. Dave, R. Bachoo, Y.T. Kim, Brain tumor genetic modification yields increased resistance to paclitaxel in physical confinement. Sci. Rep. **6**, 26134 (2016)
20. J.M. Koziara, P.R. Lockman, D.D. Allen, R.J. Mumper, Paclitaxel nanoparticles for the potential treatment of brain tumors. J. Control. Release **99**(2), 259–269 (2004)
21. M. Najlah, M. Jain, K.W. Wan, W. Ahmed, M. Albed Alhnan, D.A. Phoenix, A. Elhissi, Ethanol-based proliposome delivery systems of paclitaxel for in vitro application against brain cancer cells. J. Liposome Res. **28**(1), 74–85 (2018)
22. J. Kotera, K. Fujishige, H. Michibata, K. Yuasa, A. Kubo, Y. Nakamura, K. Omori, Characterization and effects of methyl-2-(4-aminophenyl)-1,2-dihydro-1-oxo-7-(2-pyridinylmethoxy)-4-(3,4,5-trimethoxyphenyl)-3-isoquinoline carboxylate sulfate (T-1032), a novel potent inhibitor of cGMP-binding cGMP-specific phosphodiesterase (PDE5). Biochem. Pharmacol. **60**, 1333–1341 (2000)
23. R.A. Kloner, G. Comstock, L.A. Levine, S. Tiger, V.J. Stecher, Investigational noncardiovascular uses of phosphodiesterase-5 inhibitors. Expert Opin. Pharmacother. **12**(15), 2297–2313 (2011)
24. F.A. Yafi, I.D. Sharlip, E.F. Becher, Update on the safety of phosphodiesterase type 5 inhibitors for the treatment of erectile dysfunction. Sex. Med. Rev. **6**(2), 242–252 (2018)
25. A. Dhruva, V. Hamsavardhini, S. Kamatham, A. Kataria, A. Kumar, M. Shanthi, J. Peedicayil, Avanafil inhibits the contractility of the isolated caprine detrusor muscle. Int. J. Appl. Basic. Med. Res. **9**(4), 231–235 (2019)
26. AlRuwaili, R., Al-Kuraishy, H. M., Alruwaili, M., Khalifa, A. K., Alexiou, A., Papadakis, M., Saad H.M., Batiha, G. E. S. The potential therapeutic effect of phosphodiesterase 5 inhibitors in the acute ischemic stroke (AIS). Molecular and Cellular Biochemistry, 479(5), 1267-1278. (2024)
27. A.K. Tiwari, Z.S. Chen, Repurposing phosphodiesterase-5 inhibitors as chemoadjuvants. Front. Pharmacol. **4**, 82 (2013)
28. B. Tüzün, Evaluation of cytotoxicity, chemical composition, antioxidant potential, apoptosis relationship, molecular docking, and MM-GBSA analysis of *Rumex crispus* leaf extracts. J. Mol. Struct. **1323**, 140791 (2025)
29. A.D. Becke, Density-functional thermochemistry. I. The effect of the exchange-only gradient correction. J. Chem. Phys. **96**(3), 2155–2160 (1992)
30. D. Vautherin, D.T. Brink, Hartree-Fock calculations with Skyrme's interaction. I. Spherical nuclei. Phys. Rev. C **5**(3), 626–647 (1972)
31. E.G. Hohenstein, S.T. Chill, C.D. Sherrill, Assessment of the performance of the M05−2X and M06−2X exchange-correlation functionals for noncovalent interactions in biomolecules. J. Chem. Theory Comput. **4**(12), 1996–2000 (2008)
32. S. Yokoyama, T. Kigawa, M. Shirouzu, M. Miyano, S. Kuramitsu, RIKEN structural genomics/proteomics initiative. Tanpakushitsu Kakusan Koso. Protein, Nucleic Acid, Enzyme **53**(5), 632–637 (2008)
33. K. Suzuki, J. Elegheert, I. Song, H. Sasakura, O. Senkov, K. Matsuda, M. Yuzaki, A synthetic synaptic organizer protein restores glutamatergic neuronal circuits. Science. **369**(6507), eabb4853 (2020)
34. D. Yücel, Cytotoxic effects of *Satureja cuneifolia* extract in liver cancer cell line (HepG2). Biol. Divers. Conserv. **11**(2), 42–46 (2018)
35. R. Gundogdu, M.K. Erdogan, A. Ditsiou, V. Spanswick, J.J. Garcia-Gomez, J.A. Hartley, V. Gomez, hMOB2 deficiency impairs homologous recombination-mediated DNA repair and sensitises cancer cells to PARP inhibitors. Cell. Signal. **87**, 110106 (2021)
36. M.K. Erdogan, A. Sever, R. Gundogdu, Y. Toy, I.H. Gecibesler, Y. Yapar, G. Zengin, Verbascum gimgimense, an endemic Turkish plant: evaluation of in vitro anticancer, antioxidant, enzyme inhibitory activities, and phytochemical profile. Cell Biochem. Funct. **42**(8), e70023 (2024)
37. R.D. Dennington, T.A. II, Keith, J.M. Millam, (2016). GaussView (Version 6.0.16) [Software]. Semichem Inc **13**(1)
38. M.J. Frisch, G.W. Trucks, H.B. Schlegel, G.E. Scuseria, M.A. Robb, J.R. Cheeseman, H. Nakatsuji, Uranyl extraction by N, N-dialkylamide ligands studied by static and dynamic DFT simulations. Gaussian. **09**, 9, 227 (2009)
39. I. Bhogal, V. Pankaj, V. Provaznik, S. Roy, In silico investigation of cholesterol-lowering drugs to find potential inhibitors of dehydrosqualene synthase in *Staphylococcus aureus*. 3 Biotech. **14**(2), 39 (2024)
40. Schrödinger Release 2022-4, Maestro, Schrödinger, LLC, New York, NY, 2022
41. Schrödinger Release, *Protein Preparation Wizard, Epik [Software]* (Impact, Schrödinger, LLC, New York, NY, 2021)
42. Schrödinger Release, *LigPrep [Software]* (Schrödinger, LLC. New York, NY, 2022). 2021,(nd)
43. I. Shahzadi, A.F. Zahoor, B. Tüzün, A. Mansha, M.N. Anjum, A. Rasul, M. Mojzych, Repositioning of acefylline as anticancer drug: synthesis, anticancer and computational studies of azomethines derived from acefylline tethered 4-amino-3-mercapto-1,2,4-triazole. PLoS One **17**(12), e0278027 (2022)
44. El M. Faydy, L. Lakhrissi, N. Dahaieh, K. Ounine, B. Tüzün, N. Chahboun, A. Zarrouk, Synthesis, biological properties, and

molecular docking study of novel 1,2,3-triazole-8-quinolinol hybrids. ACS Omega. **9**(23), 25395–25409 (2024)
45. Schrödinger, Release 2022-4: QikProp, Schrödinger, LLC, New York, NY, 2022
46. J.J. Chen, Y.L. Sun, A.K. Tiwari, Z.J. Xiao, K. Sodani, D.H. Yang, Z.S. Chen, PDE 5 inhibitors, sildenafil and vardenafil, reverse multidrug resistance by inhibiting the efflux function of multidrug resistance protein 7 (ATP-binding Cassette C 10) transporter. Cancer Sci. **103**(8), 1531–1537 (2012)
47. Z. Shi, A.K. Tiwari, S. Shukla, R.W. Robey, S. Singh, I.W. Kim, S.E. Bates, X. Peng, I. Abraham, S.V. Ambudkar, T.T. Talele, L.W. Fu, Z.S. Chen, Sildenafil reverses ABCB1-and ABCG2-mediated chemotherapeutic drug resistance. Cancer Res. **71**(8), 3029–3041 (2011)
48. C.M. Whitehead, K.A. Earle, J. Fetter, S. Xu, T. Hartman, D.C. Chan, W.J. Thompson, Exisulind-induced apoptosis in a non-small cell lung cancer orthotopic lung tumor model augments docetaxel treatment and contributes to increased survival. Mol. Cancer Ther. **2**(5), 479–488 (2003)
49. L. Pusztai, J.H. Zhen, B. Arun, E. Rivera, C. Whitehead, W.J. Thompson, G.N. Hortobagyi, Phase I and II study of exisulind in combination with capecitabine in patients with metastatic breast cancer. J. Clin. Oncol. **21**(18), 3454–3461 (2003)
50. A.M. Omar, A.S. Aljahdali, M.K. Safo, G.A. Mohamed, S.R. Ibrahim, Docking and molecular dynamic investigations of phenylspirodrimanes as cannabinoid receptor-2 agonists. Molecules **28**(1), 44 (2022)
51. H. Sung, J. Ferlay, R.L. Siegel, M. Laversanne, I. Soerjomataram, A. Jemal, F. Bray, Global cancer statistics 2020: GLOBOCAN estimates of incidence and mortality worldwide for 36 cancers in 185 countries. Cancer J. Clin. **71**(3), 209–249 (2021)
52. M.J. O'Connor, Targeting the DNA damage response in cancer. Mol. Cell **60**(4), 547–560 (2015)
53. A.M. Tsimberidou, E. Fountzilas, M. Nikanjam, R. Kurzrock, Review of precision cancer medicine: evolution of the treatment paradigm. Cancer Treat. Rev. **86**, 102019 (2020)
54. R.A. Weinberg, *The biology of cancer* (Garland Science, Taylor & Francis Group, LLC, 2007)
55. A.B. Chambliss, D.W. Chan, Precision medicine: from pharmacogenomics to pharmacoproteomics. Clin. Proteomics **13**(1), 10 (2016)
56. M.V. Relling, W.E. Evans, Pharmacogenomics in the clinic. Nature **526**, 343–350 (2015)
57. D.T. Wake, N. Ilbawi, H.M. Dunnenberger, P.J. Hulick, Pharmacogenomics: prescribing precisely. Med. Clin. North Am. **103**(6), 1001–1015 (2019)
58. J. Zhou, F. Zhang, J. Chen, S. Zhang, H. Wang, Chlorogenic acid inhibits human glioma U373 cell progression via regulating the SRC/MAPKs signal pathway: based on network pharmacology analysis. Drug Des. Devel. Ther. **15**, 1369–1383 (2021)
59. A. Sharma, J.J. Graber, Overview of prognostic factors in adult gliomas. Ann. Palliat. Med. **10**(1), 863–874 (2021)
60. A. Verkhratsky, A. Butt, *Glial neurobiology: A textbook* (Wiley, 2007)
61. M. Nagane, H.-J. Huang, W.K. Cavenee, Causes of drug resistance and novel therapeutic opportunities for the treatment of glioblastoma. Drug Resist. Updat. **2**(1), 30–37 (1999)
62. D.-L. Yu, Z.-P. Lou, F.-Y. Ma, M. Najafi, The interactions of paclitaxel with tumour microenvironment. Int. Immunopharmacol. **105**, 108555 (2022)
63. P.P. Ruvolo, X. Deng, W.S. May, Phosphorylation of Bcl2 and regulation of apoptosis. Leukemia. **15**(4), 515–522 (2001)
64. A.P. Nacoulma, V. Megalizzi, L.R. Pottier, M. De Lorenzi, S. Thoret, J. Dubois, O.M. Vandeputte, P. Duez, D. Vereecke, M. El Jaziri, Potent antiproliferative cembrenoids accumulate in tobacco upon infection with *Rhodococcus fascians* and trigger unusual microtubule dynamics in human glioblastoma cells. PLoS One **8**(10), e77529 (2013)
65. N.A.P. Franken, H.M. Rodermond, J. Stap, J. Haveman, C. Van Bree, Clonogenic assay of cells in vitro. Nat. Protoc. **1**(5), 2315–2319 (2006)
66. S. Wang, Y. Xiong, J. Chen, A. Ghanem, Y. Wang, J. Yang, B. Sun, Three-dimensional printing bilayer membrane scaffold promotes wound healing. Front. Bioeng. Biotechnol. **7**, 348 (2019)
67. J. Pflaum, S. Schlosser, M. Müller, P53 family and cellular stress responses in cancer. Front. Oncol. **4**, 285 (2014)
68. D. Speidel, The role of DNA damage responses in p53 biology. Arch. Toxicol. **89**(4), 501–517 (2015)
69. J. Kale, E.J. Osterlund, D.W. Andrews, BCL-2 family proteins: changing partners in the dance towards death. Cell Death & Differentiation **25**(1), 65–80 (2018)
70. E. Gorgun, A. Ali, M.S. Islam, Biocomposites of poly(lactic acid) and microcrystalline cellulose: influence of the coupling agent on thermomechanical and absorption characteristics. ACS Omega **9**(10), 11523–11533 (2024)
71. S. Karimi, L. Mafton-Azad, B. Behnajady, B. Tüzün, Response surface methodology (RSM) design to optimize the cathode of Li-ion batteries recycling in deep eutectic solvent and DFT simulation. Korean J. Chem. Eng. **42**(2), 361–381 (2025)
72. M. Akkus, M. Kirici, A. Poustforoosh, M.K. Erdogan, R. Gundogdu, B. Tüzün, P. Taslimi, (2025). Phenolic compounds: Investigating their anti-carbonic anhydrase, anti-cholinesterase, anticancer, anticholinergic, and antiepileptic properties through molecular docking, MM-GBSA, and dynamics analyses. Korean Journal of Chemical Engineering, Advance online publication. 1–20
73. D. MbomYufanyi, B. Tüzün, J.H. Nono, Y.C. Jong, J. Wirsiy, A cadmium-thiocyanate coordination polymer with bridging 2-aminopyridine: synthesis, characterization DFT studies, Hirshfeld surface analysis and docking studies. J. Mol. Struct. **1318**, 139292 (2024)
74. T. Schrader, J. Khanifaev, E. Perlt, Koopmans' theorem for acidic protons. Chem. Commun. **59**(93), 13839–13842 (2023)
75. S. Manap, H. Medetalibeyoğlu, A. Kılıç, O.F. Karataş, B. Tüzün, M. Alkan, H. Yüksek, Synthesis, molecular modeling investigation, molecular dynamic and ADME prediction of some novel Mannich bases derived from 1,2,4-triazole, and assessment of their anticancer activity. J. Biomol. Struct. Dyn. **42**(21), 11916–11930 (2024)
76. R.G. Pearson, Hard and soft acids and bases. J. Am. Chem. Soc. **85**(22), 3533–3539 (1963)
77. P.W. Ayers, An elementary derivation of the hard/soft-acid/base principle. J. Chem. Phys. **122**(14), 141102 (2005)
78. R.G. Parr, P.K. Chattaraj, Principle of maximum hardness. J. Am. Chem. Soc. **113**(5), 1854–1855 (1991)
79. A. Aksu, S. Çetinkaya, A.F. Yenidünya, ŞA. Çetinus, H. Gezegen, B. Tüzün, Immobilization of pectinase on chitosan-alginate-clay composite beads: experimental, DFT and molecular docking studies. J. Mol. Liq. **390**, 122947 (2023)
80. V. Eyupoğlu, A. Aksu, H.F. Çetinkaya, H.İ Çetintaş, S. Çetinkaya, B. Tüzün, Biosorption of dye crystal violet on *Tragopogon* sp. leaf powder: equilibrium, kinetics, thermodynamics, and DFT calculations. J. Mol. Liq. **398**, 124226 (2024)
81. J.S. Jiménez, M.J. Benítez, Gibbs free energy and enthalpy–entropy compensation in protein–ligand interactions. Biophysica. **4**(2), 298–309 (2024)
82. S. Kapancık, M.S. Çelik, M. Demiralp, K. Ünal, S. Çetinkaya, B. Tüzün, Chemical composition, cytotoxicity, and molecular docking analyses of *Thuja orientalis* extracts. J. Mol. Struct. **1318**, 139279 (2024)
83. S. Çiçek, Y.B. Korkmaz, B. Tüzün, S. Işik, M.T. Yilmaz, F. Özoğul, A study on insecticidal activity of the fennel (*Foeniculum*

vulgare) essential oil and its nanoemulsion against stored product pests and molecular docking evaluation. Ind. Crops Prod. **222**, 119859 (2024)
84. H. Medetalibeyoğlu, S. Manap, M. Alkan, M. Beytur, N. Barlak, O.F. Karataş, P. Taslimi, Novel Schiff bases: synthesis, characterization, bioactivity, cytotoxicity, and computational evaluations. Polycycl. Aromat. Compd. (2024). https://doi.org/10.1080/10406638.2024.2412217
85. M. Tapera, H. Kekeçmuhammed, B. Tüzün, S.D. Daştan, M.S. Çelik, P. Taslimi, E. Sarıpınar, Novel 1,2,4-triazole-maleamic acid derivatives: synthesis and evaluation as anticancer agents with carbonic anhydrase inhibitory activity. J. Mol. Struct. **1313**, 138680 (2024)
86. N. Abul, B. Tüzün, İ Gülçin, U. Atmaca, The synthesis of novel unnatural amino acid by intramolecular aza-Michael addition reaction as multitarget enzyme inhibitors. J. Biochem. Mol. Toxicol. **38**(9), e23837 (2024)
87. A.N. Khalilov, J. Cisterna, A. Cárdenas, B. Tüzün, S. Erkan, A.V. Gurbanov, I. Brito, Synthesis, crystal structure, Hirshfeld surface analyses, and DFT studies of (S)-2-(3,5-di tert butyl 4-hydroxyphenyl)-3,3-diethoxy-1-phenylpropan-1-one. J. Mol. Struct. **1313**, 138652 (2024)
88. M.A. Bhat, B. Tüzün, I. Koyuncu, E. Temiz, P. Taslimi, A.M. Naglah, H. Džudžević-Čančar, Synthesis, molecular modelling and choline esterase enzyme inhibitory activity of novel enaminone derivatives of sulfonamides. Bull. Chem. Soc. Ethiop. **38**(5), 1351–1368 (2024)
89. C.A. Lipinski, Lead-and drug-like compounds: the rule-of-five revolution. Drug Discov. Today Technol. **1**(4), 337–341 (2004)
90. W.L. Jorgensen, E.M. Duffy, Prediction of drug solubility from structure. Adv. Drug Deliv. Rev. **54**(3), 355–366 (2002)
91. S. Seyfi, S. Salarinejad, S. Moghimi, M. Toolabi, N. Sadeghian, B. Tüzün, A. Foroumadi, Synthesis, biological activities, and molecular docking studies of triazolo[4,3-b]triazine derivatives as a novel class of α-glucosidase and α-amylase inhibitors. Arch. Pharm. **357**(7), 2300628 (2024)
92. A. Zahirović, M. Fočak, S. Fetahović, B. Tüzün, A. Višnjevac, V. Muzika, S. Roca, Hydrazone-flavonol based oxidovanadium (V) complexes: synthesis, characterization and antihyperglycemic activity of chloro derivative in vivo. J. Inorg. Biochem. **258**, 112637 (2024)

Publisher's Note Springer Nature remains neutral with regard to jurisdictional claims in published maps and institutional affiliations.